6-2013

The Design of a Maneuverable Rolling Robot

David Carabis
Union College - Schenectady, NY

The Design of a Maneuverable Rolling Robot

By

David Carabis

* * * * * * * * *

Submitted in partial fulfillment

of the requirements for

Honors in the Department of Mechanical Engineering

UNION COLLEGE

June, 2013

ABSTRACT

CARABIS, DAVID The Design of a Maneuverable Rolling Robot. Department of Mechanical Engineering, June 2013.

ADVISOR: William Keat

The purpose of this project was to design, fabricate, and test a maneuverable rolling robot. Although some other rolling robots were researched for this project, a novel approach was taken to design a unique, cheap robot that could turn and was fully enclosed by a rotating outer shell. The design and research phase of this project included the evaluation of several designs, the development of a mathematical model detailing forward motion of the robot, and the derivation of several design equations.

Of the possible designs, an interior counterweight was chosen to provide a torque to the outside shell and move the robot forward, while a shifting internal mass was chosen to bank the robot either to the left or the right. The counterweight system applies a torque to the outer shell, and remains stationary during constant speed operation. To turn, a mass shifts to either the right or left side of the robot, changing the center of mass and causing the robot to enter a bank.

Two preliminary prototypes were constructed as a feasibility check. One prototype tested forward motion, while the other tested banking. A final, fully functional prototype was fabricated and tested. It was found that the robot satisfied all goals of the project, and could move forward with a top speed of ~6 mph, as well as turn to either the left or right.

Table of Contents

1. Introduction:

The purpose of this project is to design a maneuverable rolling robot. In the context of this project, a "rolling robot" is defined as a robot that is contained within some form of outer shell, and moves by rotating this shell. This unconventional form of propulsion creates several interesting dynamics questions to be studied: how can torque effectively be applied to the outer shell without moving or rotating the internal components, and how do different internal component weights and external shell weights affect linear acceleration and velocity.

Rolling robots have already been developed and operated successfully. For example, the spherical robot showcased in Popular Mechanics' "10 Most Brilliant Innovators of 2009" uses a "constantly shifting center of mass" for motion. This robot also stores momentum with a gyroscope system, which allows it to travel up steeper inclines than most other spherical robots [1]. Another rolling robot, Zentra's MorpHex, uses an outer shell that changes shape to push the robot forward. For example, forward motion is achieved by extending the section of the robot's shell that is at the rear contact point between the shell and the ground. This robot also has the ability to transform into a walking robot, a capability that is out of the scope of this current project [2]. These robots serve as "proofs of concept", and guarantee that constructing a rolling robot is indeed possible. However, creating a rolling robot that will reach high speeds, have good turning capabilities, and can be constructed relatively cheaply will provide many design challenges. The two spherical robots cited above were both products of extensive funding and research. It is important to note that the goal of this project is not to replicate either of

these robots, but rather to create an inexpensive and easily manufactured rolling robot that will allow the study of rolling robot dynamics.

There are several possible benefits of choosing a rolling robot over more conventional transportation designs. For one, having the outer shell of the robot act as the rotational surface guarantees that the "wheel diameter" is as large a portion of the total height of the robot as possible. A larger wheel diameter results in a higher linear velocity for a given angular velocity. In the case of a spherical robot, one possible design choice, the "wheel component" (the sphere) has no bias towards any direction. This is beneficial for maneuverability, and would allow for a change of direction without any changes to wheel orientation. A rolling design would also provide a large amount of stability, since there is no inherent external top or bottom. This lack of a top or bottom portion of the shell means that the robot can never be flipped, and will always land in a sufficient orientation when dropped.

The analysis of this robot involved creating mathematical models and computer simulations. Design equations were derived from basic mechanics principles, and used to size motors and counterweights for the system. This portion of the analysis was useful during the design phase, and is outlined in Chapter 6. A full mathematical model for forward motion was also derived, which will be implemented in the MATLAB sub-program Simulink in future work. Results from this simulation can then be compared with results from a prototype robot, and, in turn, the simulation can be refined to match the actual dynamics of a rolling robot. Having an accurate simulation available will allow for the effects of different parameters to be tested without the construction of additional prototypes. This model is described in detail in Chapter 5.

A fully functional prototype robot was designed and constructed for this project. This prototype was able to move forward and backward, and has the ability to turn left and right. The prototype is controllable via RC, which gives the user full control over the robot's movements. Although this method of control poses some challenges, it allows the user to quickly explore a wide range of operating conditions and situations. Future work could use feedback loops and control boards to mitigate unwanted motion or acceleration, making the robot easier to operate and far more user-friendly. Chapter 7 discusses the detailed design of this robot, while Chapter 8 is an evaluation of the robot's performance.

2. Design Criteria:

2.1 Overview

The design criteria for the final robot can be broken into two subsets: critical constraints and goals. Critical constraints are design criteria that are considered necessary for the success of this project; without these constraints, the robot could not operate as a fully functional rolling robot. Goals are not necessary for the successful operation of the rolling robot, but are rather measurements of the rolling robot's performance. For example, if the robot could not meet the speed goal but could still travel forward the robot would be meeting the critical constraints, and therefore fully operational. How close the robot's top speed matches the previously set goal then serves as a quantifiable measurement of performance.

2.2 Critical Constraints

- Rolling – The robot must use a rolling outer-shell for motion. This shell does not necessarily have to be spherical in shape.
- Maneuverability – The final design of the robot should be able to move forward and backward, and have some form of turning mechanism.
- Containment – The robot must be self-contained within its rolling shell.
- Cost – The robot must stay within budget, excluding any scavenged parts.
- Control – The robot must have the ability to be controlled via basic remote control.

- Materials – The materials must be able to withstand a reasonable amount of use. These material choices should weigh weight, durability, and cost against one another.

2.3 Goals

- Speed – The robot can obtain speeds of 10 miles per hour in a straightaway.
- Acceleration – The robot can reach top speed in less than 5 seconds.
- Maneuverability – The robot has a turning radius of 6 inches or less at a standstill and a turning radius of 8 feet at top speed.
- Cost – The entire cost of the robot is less than $500.00 including scavenged parts.
- Geometry – The robot can fit within a 1.5 foot cube.

3. Initial Design Concepts:

3.1 2-Wheeled Cylinder

This concept consists of a cylindrical outer shell that is divided in half. Each half of the outer shell acts as a wheel and operates independently of the other. The independence of these two wheels allows for a zero-point turning radius when the robot is at a standstill. This zero-point turn is executed by spinning the wheels in opposite directions, as illustrated in Figure 1. This system would rely on two high precision motors to maintain a straight path of movement when travelling forward or backward. To travel either forward or backward in a straight line, both wheel motors must turn at the same angular velocity. If the two motors have low precision and output different torques or angular velocities at the same input voltage, the robot would turn slightly right or left instead of travelling forward or backward as desired. The 2-wheeled cylinder shell design is shown below in Figure 2.

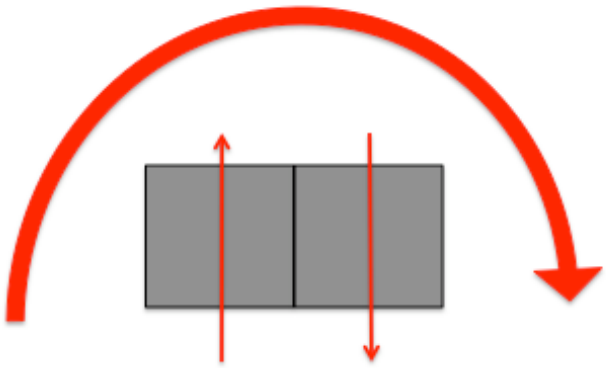

Figure 1: Zero-point turning method for two-wheeled concept (top view of robot).

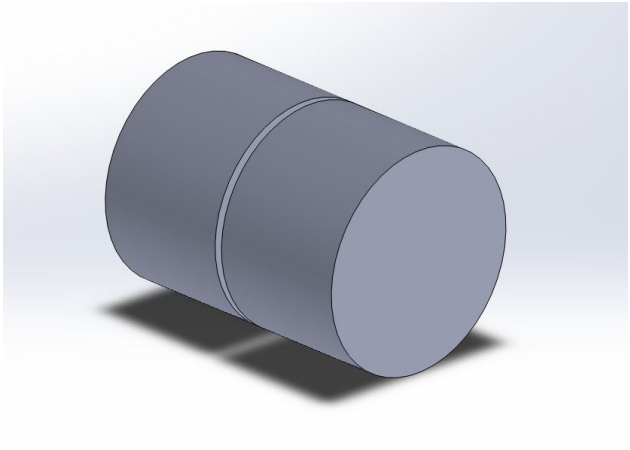

Figure 2: Sketch of the 2-wheeled cylinder design.

3.2 2-Wheeled Sphere

This concept is similar to the 2-wheeled cylinder concept with the exception that the outer shell is a sphere rather than a cylinder. Like the 2-wheeled cylinder concept, this design would have a zero-point turning radius at a standstill, but may have trouble turning at higher speeds. However, the spherical design would allow for a secondary turning mechanism that uses a shifting center of mass to be added. This type of turning mechanism would, in theory, cause the robot to bank and could be used at relatively high speeds. Like the previously discussed design, both motors spinning in the same direction would provide straight forward or backward motion, while counter-spinning motors would provide a zero-point turn. This design would also require a high amount of precision in the two wheel motors to ensure a straight line of forward motion. Care would have to be taken to ensure the internal center of mass is oriented so each of the two

hemisphere wheels have equal contact with the ground. The 2-wheeled sphere shell design is shown below in Figure 3.

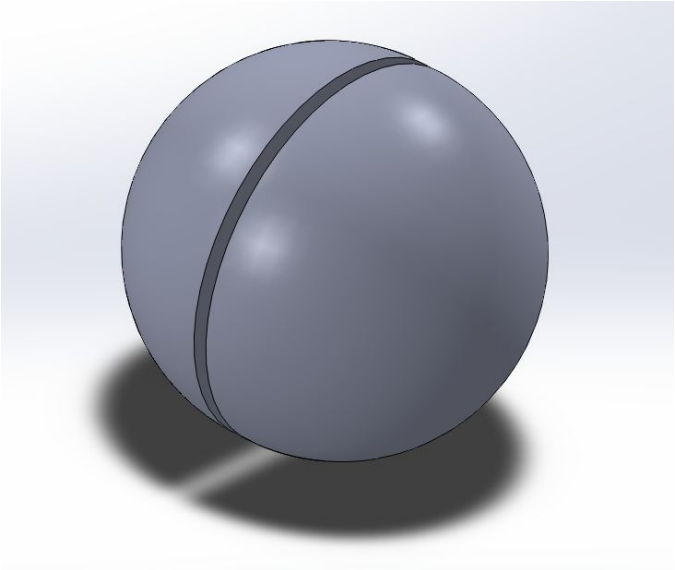

Figure 3: Sketch of the 2-wheeled sphere design.

3.3 Uni-Shell Sphere

This design incorporates a solid, unified outer shell. There is no inherent zero-point turning mechanism in the solid shell, so this design will either not have this capability or must rely on another system to provide zero-point turning. One system that could provide zero-point turning would be a quickly spinning mass that spins perpendicular to the ground. The angular acceleration and moment of inertia of the mass would exert a torque against the outer shell and other internal components, spinning the entire robot in one direction. Some major concerns associated with using this system for a zero-point turn are repeatability and accuracy. However, these concerns may be mitigated through the use of precise and accurate motors to turn the mass. The same shifting center of mass system discussed in the previous design could also be used to provide banking at

higher speeds. Care must be taken to orient the internal center of mass correctly in this system, so that forward motion occurs in a straight line. Unlike the previously discussed designs, this design features a single drive motor for forward and backward motion. To travel in a straight line, this single motor spins with the internal components remaining stationary and the outer shell rotating. See Figure 4 below for the shell design of this concept and a concept drawing of the internal components.

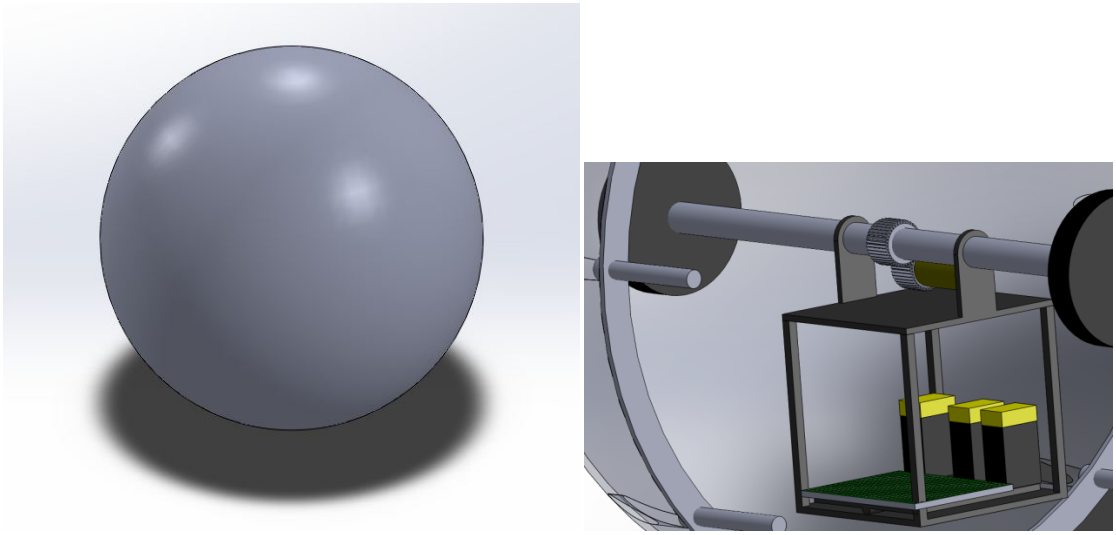

(a) (b)

Figure 4: (a) Sketch of the uni-shell sphere design. (b) Close up of internal components.

4. Evaluation of the Uni-Shell Sphere Concept:

4.1 Results of Preliminary Prototyping

All of the design concepts proposed for this robot use an internally applied torque applied to an outer shell to provide forward motion. Since the exact nature of this method of movement can be hard to conceptualize without extensive modeling or research, an inexpensive prototype was constructed from scrap materials. This prototype was constructed to ensure that this method of propulsion would work, and to see if the internal components would stay stationary during forward movement. The prototype was constructed from the bottom portion of a plastic container, a small motor, a motor shaft, a battery pack, and a switch. The battery pack and motor act as the internal counterweight mass and, in theory, will provide the reaction torque needed to spin the outer shell. See Figures 5 and 6 below for a schematic of the system and photographs of the finished preliminary prototype.

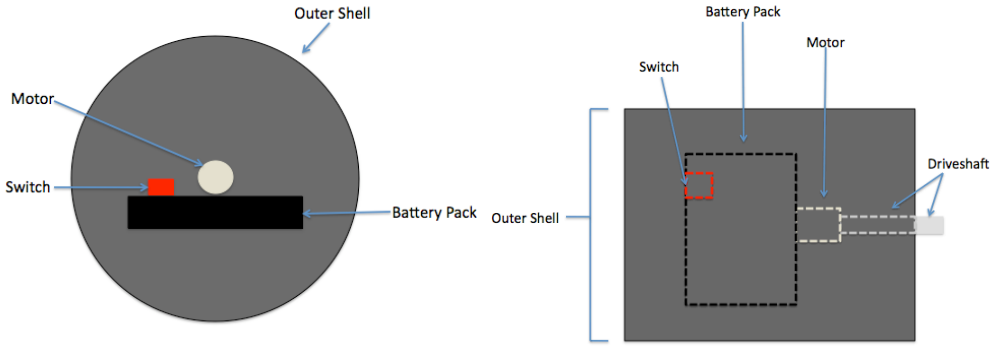

(a) (b)

Figure 5: (a) Side view schematic. (b) Top view schematic.

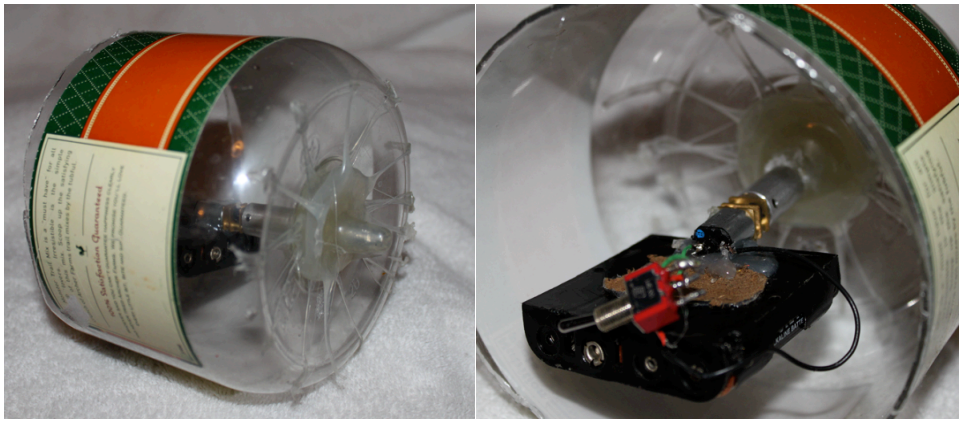

(a) (b)

Figure 6: (a) Photo of preliminary prototype. (b) Photo of internal components.

The prototype model could travel forward in a relatively straight path, but lacked the capability to start forward motion on its own. Pushing the prototype at the correct moment would start forward motion, after a small transient period where the internal mass would continue to rotate slightly. Prior to travelling forward the internal mass would rotate and the outer shell would stay relatively stationary or rock slightly from side to side. It was hypothesized that the inability to start linear motion was a result of either insufficient output torque to start movement or shell deformation, and that this problem could be solved by using a larger motor and a more rigid outer shell. Weights were added to the internal components to see if a difference in mass would affect startup, but no observable difference was noted. This was done to ensure enough internal mass was available to provide the largest reaction torque possible on the outer shell. If, for example, the internal mass was much smaller than the weight of the external shell, it would be easier for the motor to spin the internal mass rather than the outer shell. A series of speed tests were also conducted, and an average top speed of approximately 2.2 miles per hour was measured. See Appendix A for speed test experimental data.

Another preliminary prototype was created to simulate the banking system previously described. A small steel shaft was attached to a hamster ball to simulate a drive shaft running through the center of a spherical robot. Scale weights were attached around this drive shaft, and distributed so that more weight was located in either the left or right hemisphere. This ball was then pushed by hand, and observations about the ball's forward motion were made. The ball was shown to bank either left or right, depending on the distribution of the internal mass. Figure 7 shows one half of the ball and an internal view of the ball, both with unevenly distributed scale weights attached.

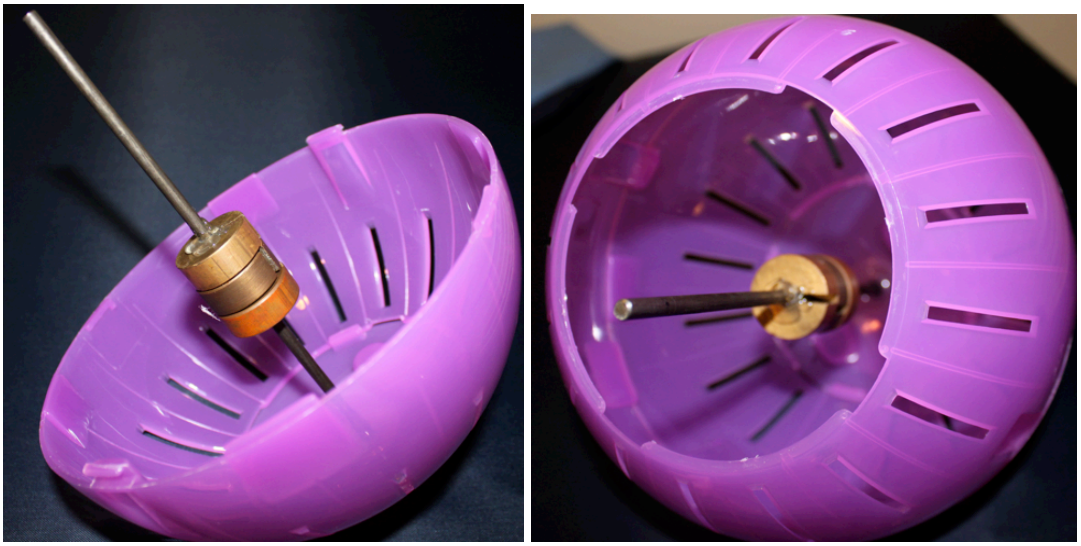

(a) (b)

Figure 7: (a) Half of the hamster ball used in the banking experiment (b) Internal view of the hamster ball setup

4.2 Selection of the Uni-Sphere Concept

The success of the two preliminary tests described in this section led to the uni-sphere concept being deemed not only feasible, but also likely to succeed. The success of the banking test also led to the two-wheeled designs, which would have relied upon two high-precision motors, being deemed unnecessary. This combination of results, as well as

the overall simplicity of a single shell design, resulted in the selection of the uni-sphere concept as the most promising. From this point forward, all analysis and design was constrained to this concept.

5. Dynamic Model of Forward Motion:

5.1 Free Body Diagrams

The development of a mathematical model started with the creation of free body diagrams for both the external shell and the internal components of the rolling robot. These free body diagrams account for both external forces and the forces and torques between the two components. It is important to note that the free body systems were treated as two-dimensional, the center of mass for the external shell was assumed to be at the center of the shell, and the center of mass for the internal components was assumed to be offset from the attachment point by some distance. A sketch of the entire system is shown in Figure 8, which depicts the outer shell, internal components, and positive rotational directions for both. The free body diagrams of the external shell and internal mass are shown in Figures 9 and 10, respectively. In both of these free body diagrams O_x and O_y represent reaction forces at a pin joint on the central axis of the outer shell. A weight force and the motor torque are also depicted in both free body diagrams. In Figure 9, a normal force due to the ground is acting on the bottom of the shell. In Figure 10, point *c* is the center of mass for the internal component.

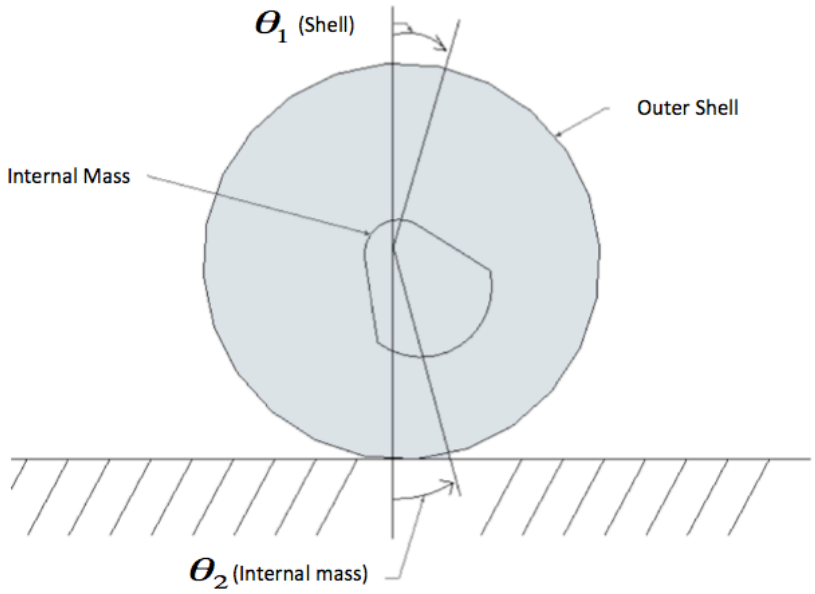

Figure 8: Sketch of rolling mechanism.

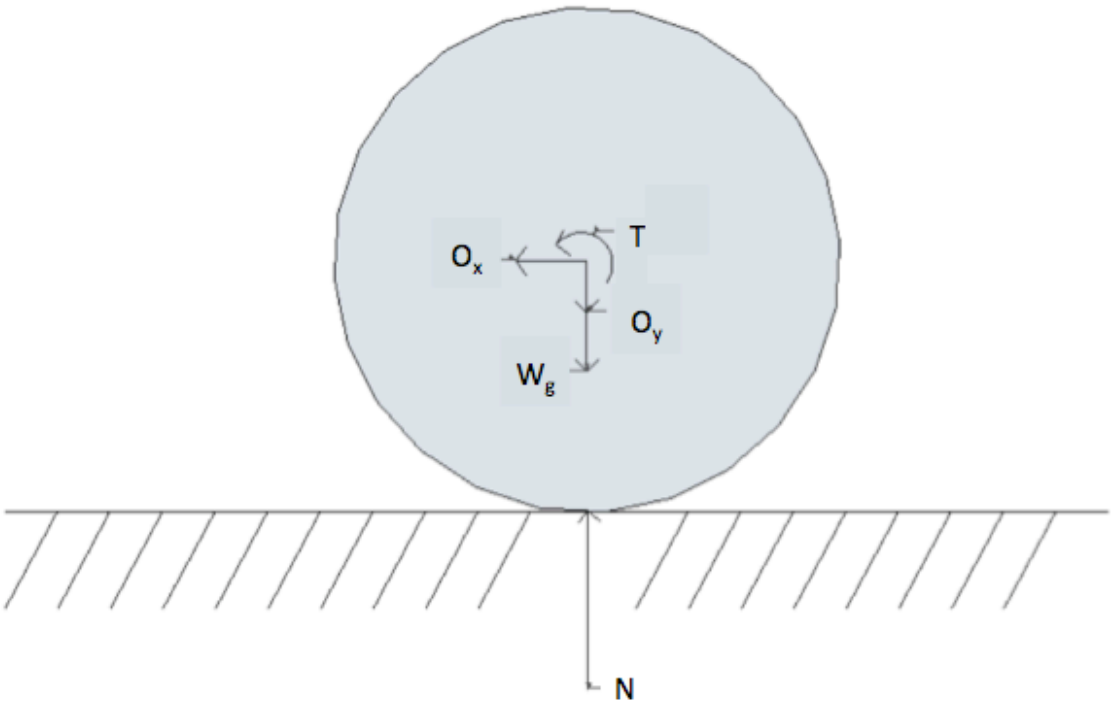

Figure 9: External shell free body diagram.

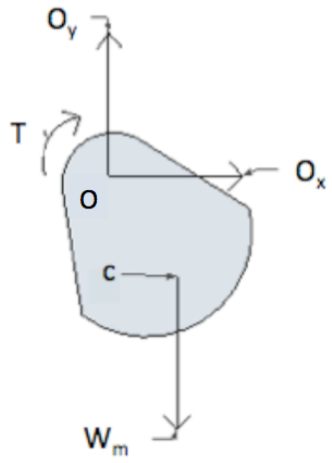

Figure 10: Internal mass free body diagram.

5.2 Derivation of the Governing Differential Equations

The mathematical model for forward motion sought to model the angular displacement, velocity, and acceleration of both the external shell and internal mass.

The first step in the model derivation was to write Newton's second law for the internal mass. Referencing Figure 9 and summing forces, we obtain:

$$\sum F_x = m_2 a_{cx} \qquad O_x = m_2 a_{cx} \tag{1}$$

$$\sum F_y = m_2 a_{cy} \qquad O_y - m_2 g = m_2 a_{cy} \tag{2}$$

where O_x and O_y represent the components of force exerted by the outer shell on the motor shaft at O, a_{cx} and a_{cy} define the acceleration of the center of mass at c, m_2 is the internal mass, and g is the acceleration of gravity. Rotational equilibrium of the internal mass was examined by summing moments about its center of mass, c:

$$\sum M_c = J_2\ddot{\theta}_2 \qquad T - O_x r\cos\theta_2 - O_y r\sin\theta_2 = J_2\ddot{\theta}_2 \tag{3}$$

where T is the torque applied by the motor, r is the distance between points O and c, θ_2 is the angular displacement of the internal mass, J_2 is the moment of inertia of the internal mass with respect to c, and $\ddot{\theta}_2$ is the angular acceleration of the internal mass.

The accelerations in equations (1) and (2) can be rewritten in terms of the angular displacements and their derivatives. To do so, we first relate the absolute acceleration of the point c to the absolute acceleration of point O by introducing the following relative acceleration equation:

$$\vec{a}_c = \vec{a}_O + \vec{a}_{c/O} \tag{4}$$

in which $\vec{a}_{c/O}$ is the acceleration of point c relative to O. Replacing $\vec{a}_O$ by the expression for linear acceleration of a rolling cylinder, and $\vec{a}_{c/O}$ by the general kinematic expression for acceleration of a point on a rotating body, leads to:

$$\vec{a}_c = R\ddot{\theta} + (\ddot{\theta}_2\hat{k}\times\vec{r}_{c/O}) + \dot{\theta}_2\hat{k}\times(\dot{\theta}_2\hat{k}\times\vec{r}_{c/O}) \tag{5}$$

where R is the radius of the outer shell and the position vector $\vec{r}_{c/O}$ directed from O to c is given by:

$$\vec{r}_{c/O} = r\sin\theta_2\hat{i} - r\cos\theta_2\hat{j} \tag{6}$$

Performing the cross products implied by (5), and then substituting into equations (1) and (2), results in the following expressions for the reaction forces at O:

$$O_x = m_2\left(R\ddot{\theta}_1 + r\ddot{\theta}_2\cos\theta_2 - r\dot{\theta}_2{}^2\sin\theta_2\right) \tag{7}$$

$$O_y = m_2\left(g + r\ddot{\theta}_2\sin\theta_2 + r\dot{\theta}_2{}^2\cos\theta_2\right) \tag{8}$$

If we now substitute equations (7) and (8) into equation (3), we obtain the following differential equation governing the rotational motion of the internal mass:

$$T - (R\ddot{\theta}_1 + r\ddot{\theta}_2 \cos\theta_2)m_2 r\cos\theta_2 - (g + r\ddot{\theta}_2 \sin\theta_2)m_2 r\sin\theta_2 = J_2\ddot{\theta}_2 \tag{9}$$

Moment equilibrium of the outer shell with respect to *O* yields a second differential equation, this one governing the rotational motion of the outer shell:

$$T = J_1\ddot{\theta}_1 \tag{10}$$

where J_1 is the mass moment of inertia of the outer shell with respect to *O*.

Together, equations (9) and (10) define a coupled system of differential equations in terms of the forcing function *T*. See Appendix B for a list of symbols used in this mathematical model.

5.3 Formulation of the Simulink Model

The MATLAB sub-program Simulink was used to run simulations of the mathematical model for forward motion. These simulations will allow changes in system parameters, such as counterweights or motor sizes, to be studied without extensive prototyping. This model was designed by rewriting the mathematical model as an equation equal to $\ddot{\theta}_2$. Integrator blocks then were used to simulate angular speed and displacement ($\dot{\theta}_2$, θ_2), which were looped through the simulation and directed back to $\ddot{\theta}_2$ through sum and multiplication blocks. These blocks make up the "equation" that is equal to $\dot{\theta}_2$. See Appendix C for the simulation model.

6. Design Methodology:

6.1 Brief Overview

A number of equations were derived during the design phase to size a specific component or study one sub-system independently of the entire robot. These design equations were used primarily to size motors, servos, and counterweights for the system. In addition, these equations also served as a feasibility study; if any of the obtained values were unreasonable, a different design approach may have been taken. It is important to keep the performance requirements in mind while reviewing these design equations: the robot must have the ability to travel forward and backward without excessive movements of the internal counterweight system, and the robot must be able to bank or turn.

6.2 Design Equations for Forward Motion

One continuous rotation motor and one inertial mass counterweight are required for forward motion. Since the size and shell of the robot has already been determined, both the necessary motor requirements and the necessary counterweight inertial mass can be considered functions of the shell size, shape, and weight, as well as other specified design requirements. Both the required torque and required power were calculated and then compared to available motor specs. Motors were deemed viable options if the maximum power and half of the stall torque exceeded the power and torque requirements. Since maximum power for a motor is not always listed, the following equation was used to calculate maximum power:

$$P_{max} = \frac{1}{4} T_{stall} \omega_{noload} \tag{11}$$

where P_{max} is the maximum power of the motor, T_{stall} is the stall torque of the motor, and ω_{noload} is the no-load angular velocity of the motor. The required torque was found using the equation:

$$T_{req} = I_c \alpha \tag{12}$$

where T_{req} is the required torque, I_c is the inertial mass moment of the external shell, and α is the angular acceleration required. Angular acceleration was treated as a design requirement, and was set at 5 s^{-2} (this value corresponds to the robot reaching top speed at 5 seconds; this value was chosen arbitrarily). The following equation was used to find the maximum power:

$$P_{req} = T_{req} \omega_{max} \tag{13}$$

where P_{req} is the required power and ω_{max} is the maximum angular velocity.

Design equations were also developed to size the necessary internal counterweight mass. A diagram of the internal components (modeled as a pendulum and weight) was set up as shown in Figure 12. The pendulum is set up so that the pivot point corresponds to the drive shaft attachment point of the internal components. This diagram models the internal components as a point mass located at the end of the pendulum. As the angle of deflection increases, the torque applied on the driveshaft by the pendulum increases. The following equation was used to find theoretical lower and upper bounds of necessary counterweight size:

$$T = m_1 g \sin \varphi r \tag{14}$$

where T is either the required or stall torque, g is the acceleration of gravity, φ is the angular displacement of the pendulum, m_1 is the mass of the internal components, and r is the distance between the point mass and the driveshaft. The reasoning behind this

equation is that the motor will reach stall torque after rotating the internal mass a certain angular distance, and at this point all of the applied torque will be transferred to rotating the external shell. The angular displacement φ is treated as a design requirement, with smaller values requiring larger counterweight masses. To find the upper bound mass requirement (that is, the maximum mass needed to transfer all of the motor torque to the external shell for a given angular displacement), T was set equal to the motor stall torque. To find the lower bound mass requirement (that is, the mass requirement where the inertial mass of the internal components matches that of the external shell), T was set equal to the required motor torque. It was concluded that the required mass for successful operation would lie somewhere between these two mass values, and could be precisely determined through experimentation and testing.

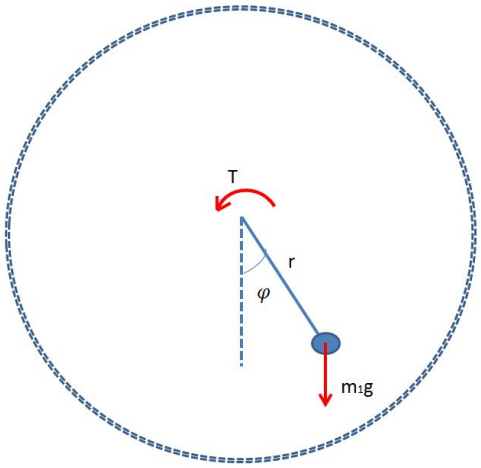

Figure 12: Diagram used for counterweight design equation.

6.3 Design Equations for Turning

A similar set of design equations were derived for the banking mechanism. These equations sought to size the servo motor and the weights necessary to create a sufficient

bank. Since the servo motor would move the banking weights, the weight sizing equations were derived and solved first. These equations were derived from a free body diagram featuring the external sphere, the offset mass used for turning, and the motionless counterweight. This free body diagram is shown in Figure 13, which shows both the weight forces and centrifugal forces of the different components. In the diagram, w corresponds to the weight force, m corresponds to the mass of a component, P represents the turning radius of the robot, and ω represents the angular velocity of the robot. The subscripts 1, 2, and 3 correspond to the motionless counterweight, the external shell, and the offset turning mass, respectively.

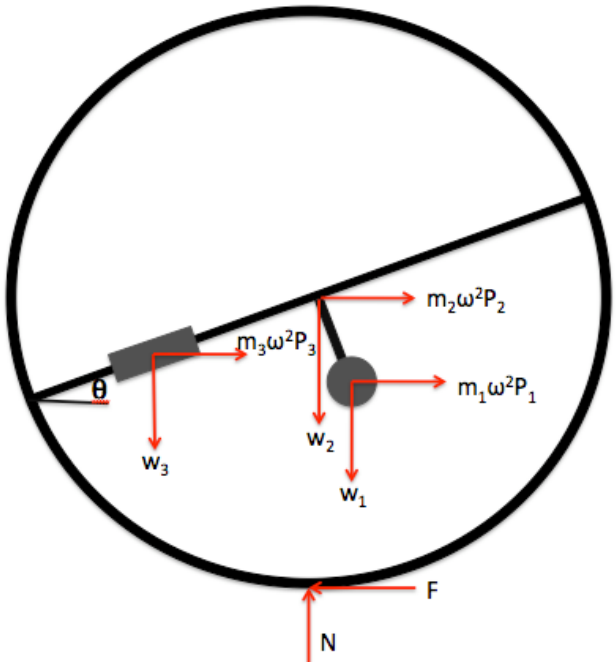

Figure 13: Free body diagram for banking scenario.

To find the necessary turning mass, m_3, a desired turning radius, P, at a desired angular velocity, ω, was chosen. The following equation was used to solve for the angular displacement, θ:

$$P = \frac{R}{Tan\theta} \tag{15}$$

where R is the radius of the sphere. After θ has been found, summing the moments about the center of the sphere can be used to find m_3. These equations ensure that the required mass counteracts the centrifugal forces the robot will experience while turning during forward motion.

The servo motor was sized using the equation:

$$T_{req} = mgd \tag{16}$$

where m is the offset turning mass, and d is the diameter of the gear used to shift the mass either left or right. This equation accounts for the "worst case scenario", where the ball has turned so that the driveshaft is perpendicular to the ground and the servo motor must hold the offset mass against gravity.

6.4 Results for Current Design

A top linear speed of 10 mph and an angular acceleration of 5 s^{-1} were chosen for sizing the drive motor. These values result in a required torque of 0.135 lb ft and a required power of 3.59 W. A Polulu 37Dx54Lmm 50:1 gear-motor (part no. 1104) was chosen for the final design. This motor exceeds both the required torque and power, with half of the stall torque listed as 0.443 lb ft and the maximum power calculated to be 6.29 W. It should be noted that the actual top speed and angular acceleration are expected to be lower than these values, due to friction and other unforeseen losses.

The lower and upper bound counterweight masses for forward motion were calculated to be 2.5 lb and 16.4 lb for an angular displacement of 15°. These values were obtained by using the stall torque for the #1104 Polulu gear-motor. This calculation

shows that the maximum mass needed is a reasonable number. If this maximum required mass were much larger, say an order of magnitude larger, a question of feasibility would arise.

A turning radius of 10 ft at a linear velocity of 5 mph was chosen for the offset turning mass calculations. These calculations led to an estimated 2 lb mass needed to turn the robot at the specified speeds. Once again, actual performance is expected to be lower than predicted by these equations. However, a 2 lb mass appears to be a reasonable turning mass in terms of fitting said mass inside of the internal counterweight system. This mass estimate led to a required servo-motor torque of 0.333 lb ft for a 2 in diameter gear, well within the chosen Futaba S3004 servo's capabilities.

7. Detailed Design:

7.1 Overview of the Final Design

The final design of the rolling robot features a unified, spherical outer shell with internal components acting as a counterweight for forward and reverse motion. The internal counterweight is attached to the driveshaft by two pillow-block ball bearings, with the motor coupled to the driveshaft via two gears. Two small masses that make up the offset turning mass are mounted on a flat piece of ABS plastic that is shifted either left or right by a servo. This servo drives the ABS piece via a gear and rack. The final design also uses two battery packs: a 12V NiMH pack used for forward and backward motion, and a 6V NiCd pack used for powering the servo and radio control receiver. Figure 14 shows the completed Solidworks model of the final design, and Figure 15 is a photo of the completed robot. See Appendix E for technical drawings of the design.

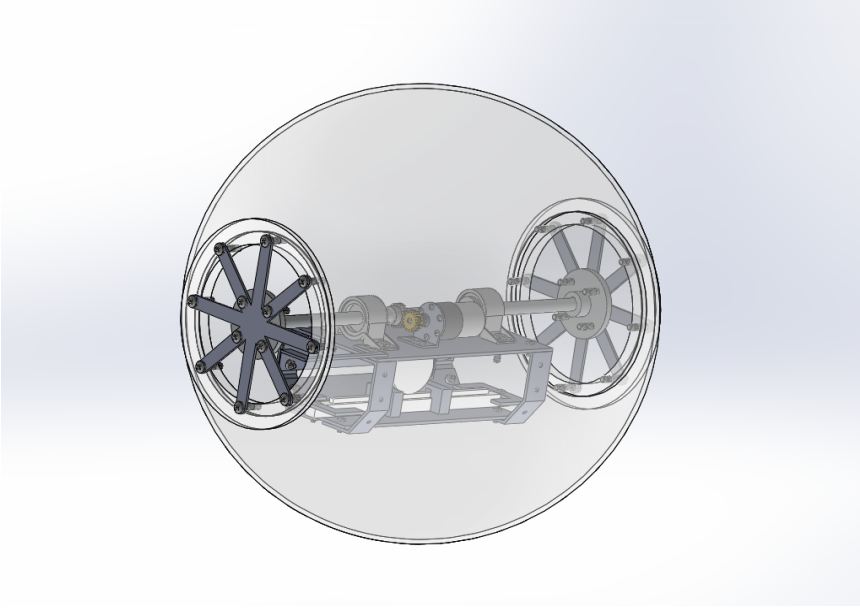

Figure 14: Solidworks model of completed design.

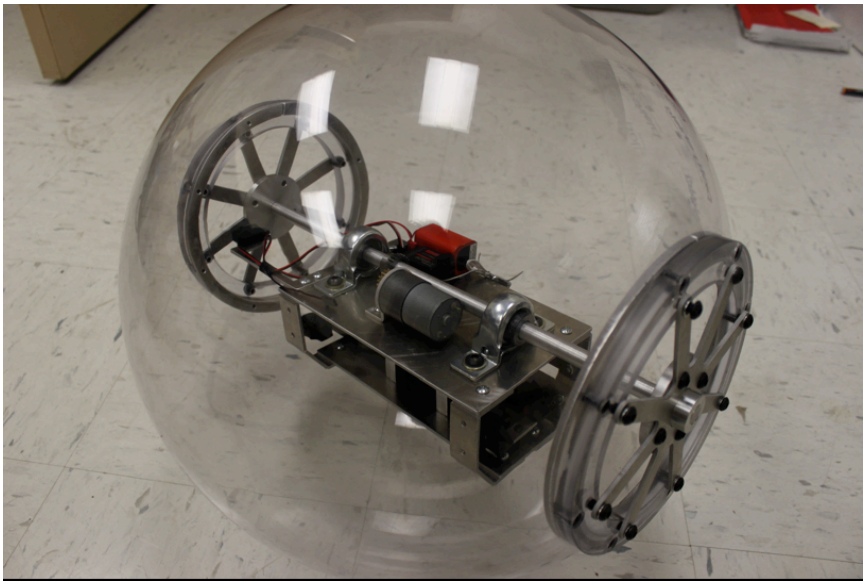

Figure 15: Photo of the completed robot.

7.2 Drive Mechanism

The drive mechanism is composed of an aluminum driveshaft and a Polulu #1104 motor. These two components are joined together by two gears with nearly similar teeth numbers. Since the Polulu motor has an attached gear box, a 1:1 or nearly 1:1 gear ratio was desired between the driveshaft and the gear motor output. Two pillow block ball bearings attach the driveshaft to the carriage plate. The undercarriage is then attached to this carriage plate using four mounting brackets. The 12V battery and turning mechanism are located within the undercarriage, while the 6V battery and radio transceiver are attached atop the carriage plate. These components were fastened to the robot using industrial strength Velcro. Figure 16 shows a close up view of the drive mechanism.

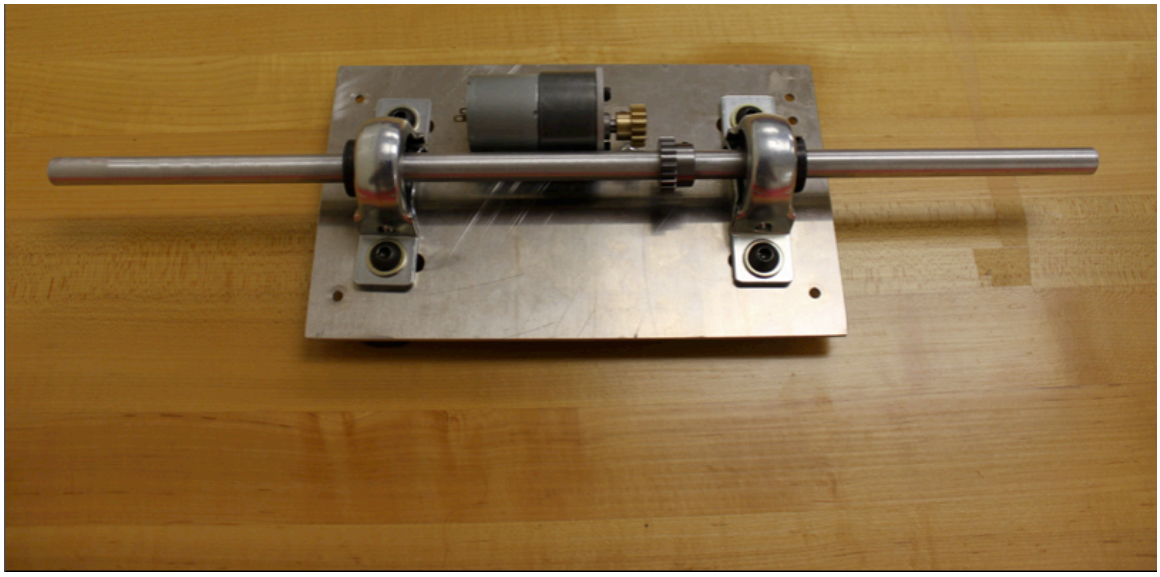

Figure 16: Drive mechanism (excluding electronic components).

The drive mechanism is rigidly attached to the shell by two mounting plates. The original design called for the polycarbonate plates to be glued to the shell, but issues that arose during the fabrication phase led to the polycarbonate plates being bolted into the shell. This rigid connection allows the driveshaft to rotate the outer shell without any flexibility or give.

7.3 Banking Mechanism

The banking mechanism, located within the undercarriage, consists of a servo-motor, a gear, a rack, rack mounts, and two weights. It is important to note that the Futaba servo used for the turning mechanism was modified so that it could turn approximately 180°, giving the rack a full travel of about 2 inches in either direction. The rack is composed of a small plastic gear rack and a larger square-stock piece of ABS plastic. ABS plastic was chosen for its low frictional coefficient, as the rack slides across

the aluminum undercarriage plate. Two rack mounts stop the rack from moving upwards or laterally. Industrial grade Velcro was used to attach the turning weights to either end of the rack. This allows for adjustability and the testing of various turning mass sizes. Figure 17 shows the banking mechanism located inside the undercarriage.

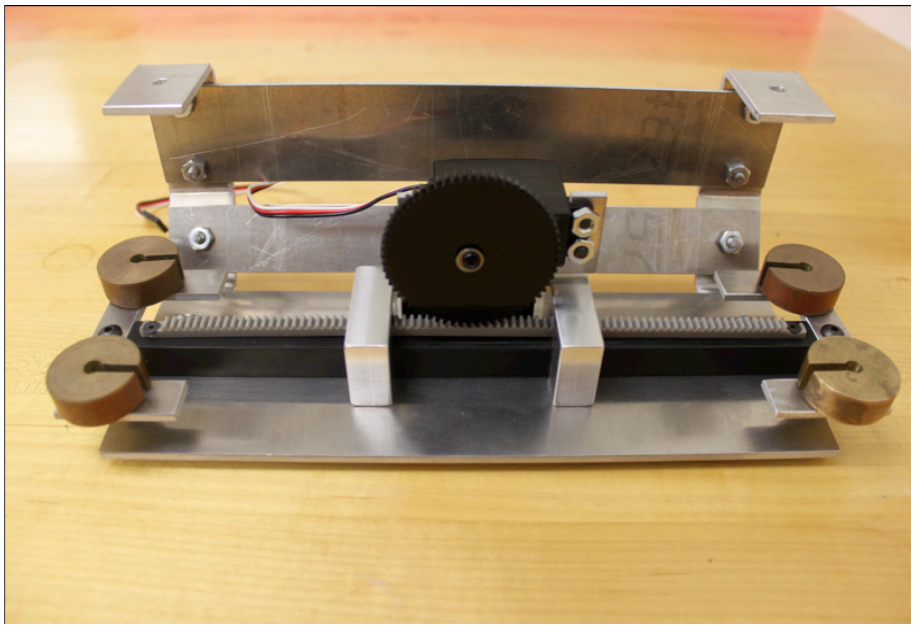

Figure 17: Banking mechanism located inside the undercarriage.

7.4 Electronic Design

Two circuits were used in the final design: one for the driveshaft motor, and one for the radio transceiver and servo control. These two circuits were not integrated with one another due to the differing voltage and power requirements of the drive motor and banking servo. A FingerTech tiny ESC motor speed controller was integrated into the drive motor circuit to provide speed control and reverse direction for the drive motor. It should be noted that the battery elimination circuit located on the speed controller was not used. This BEC was designed to run a radio transceiver at approximately 5V, but

could not provide the amperage to operate the servo sufficiently. A wiring diagram is shown in Figure 18.

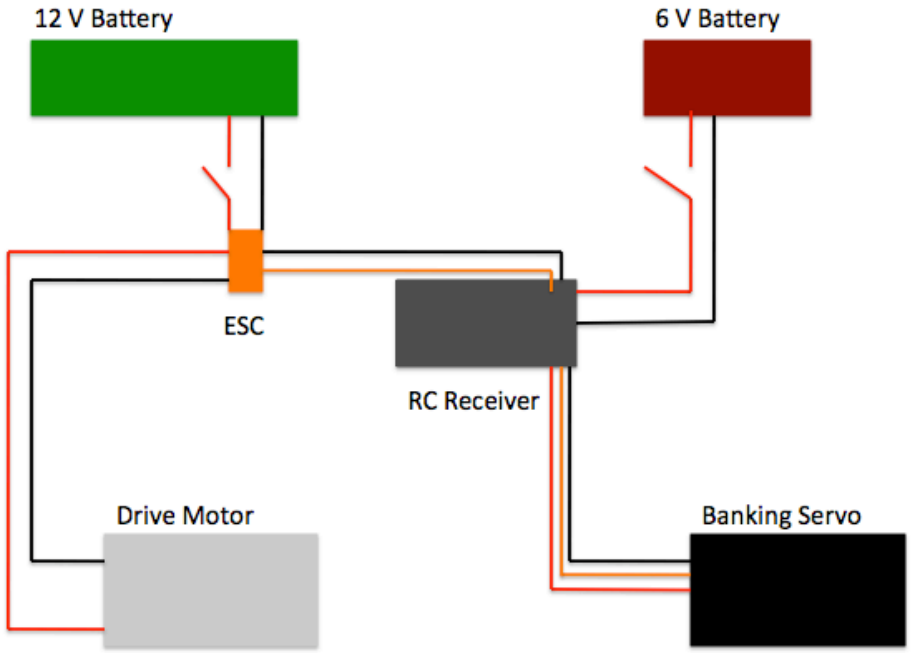

Figure 18: Wiring diagram (red wires- power; black wires- ground; orange wires- signal).

7.5 Notes on Fabrication

The fabrication of the final robot matched the technical drawings presented in Appendix E invariably, with exception to the polycarbonate plates mounted to the shell. These plates had been designed to be glued to the sphere, but it was found that the shell was not perfectly spherical and the design had to be altered. Aluminum plates, to which the polycarbonate plates were bolted, were placed inside the shell. In essence, the polycarbonate plates and new aluminum plates "sandwich" the edges of the shell, with the bolt holes running through the shell to provide rotational stability.

Due to the nature of the design, a method had to be developed to accurately cut two matching holes in either side of the sphere. The machinists at Union College devised a method that uses two plywood plates, both with holes and fillets that match the diameter of the sphere, to hold the sphere securely in place. These plywood plates are fastened to one another using long threaded rods. This setup was then placed inside a CNC machine, and the two holes were accurately machined in the polycarbonate sphere. Figure 19 shows this setup.

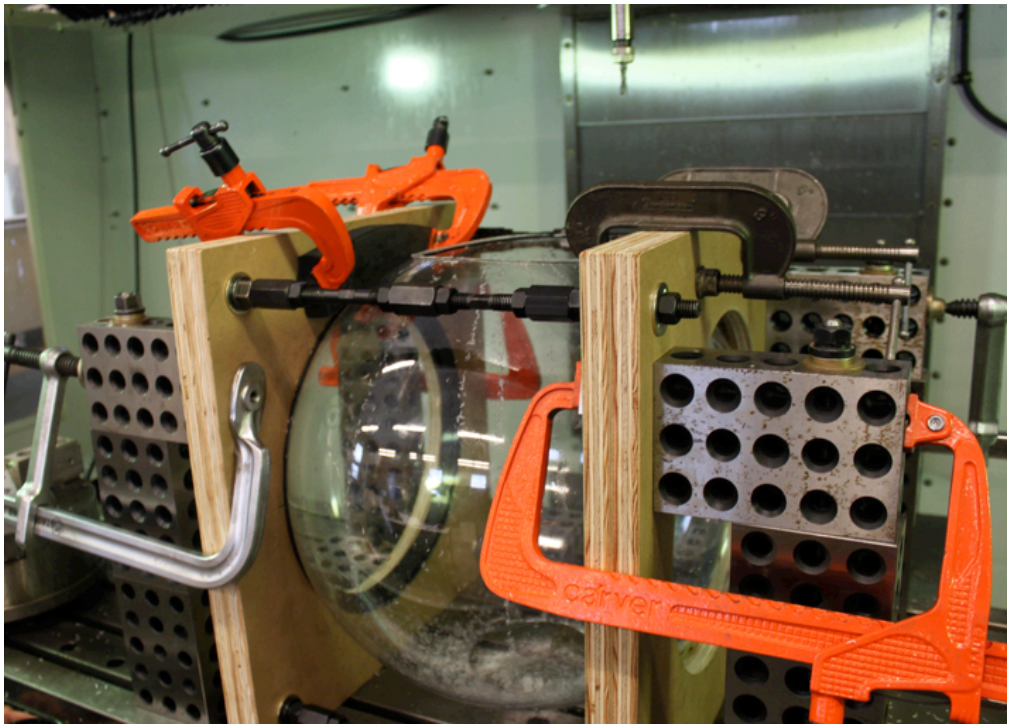

Figure 19: Novel setup used to cut holes in plastic shell.

It should also be noted that aluminum plate was used for all metallic plates in the design (such as the carriage and undercarriage plates). The weight reduction offered by choosing aluminum over steel was considered a benefit after testing the completed robot,

since there is sufficient space within the undercarriage to add additional weights if needed.

8. Evaluation of Performance:

Testing of the completed robot showed that the robot could be moved forward and backward successfully, as well as bank either left or right. Even though all of these functions could be carried out via RC, continued use often resulted in instability, with the robot "wobbling" left and right. It was observed that this "wobble" could be counteracted by shifting the turning mass either left or right, leading to the conclusion that this instability could be counteracted with some form of control method. It was also observed that if the robot tried to accelerate too quickly, the internal components could rotate excessively within the shell. Although this was possible, it was relatively easy for an operator to control forward or backward motion. It was sometimes difficult to slow or stop the robot, which is another function that may greatly benefit from some form of control system. Overall, the robot was considered controllable via RC, at least after some operation practice. Since all of the critical constraints were satisfied, this prototype was considered a success.

Video footage of the robot taken during testing was also used to estimate the top speed of the robot. A top speed estimate of ~6 mph was obtained from the footage. Acceleration and turning radii were difficult to discern from the footage, so continued testing is needed to determine these values. Continued testing could also yield a more accurate speed estimate.

9. Conclusions:

In conclusion, the outcome of this project is considered a success. All of the critical constraints were met, and the performance of the robot met, if not exceeded, the expectations of those involved in the project. However, this does not mean there is not room for improvement, or that controlling the robot is easy or user friendly. The next step in the development of this robot could be the addition of onboard controllers. These controllers could use feedback loops to prevent unwanted acceleration in the internal counterweight system, or use the shifting internal mass to counteract the observed "wobble". Another possible solution to this instability is the addition of gyroscopes, which could help maintain rotational inertia during use.

The possible addition of feedback control loops has also led to the first proposed application of this robot: as a teaching tool. If feedback loops were successfully integrated, future students could alter or remove these feedback controls to observe the effects of different controls on a system. Direct control of the system has shown that the robot can act both stably and unstably, so there is potential for the study of both cases.

Appendix A – Forward Motion Experiment Data

The objective of this test was to determine the steady-state speed of the preliminary prototype robot, as well as testing the feasibility of an internal counterweight rotating an external shell. Knowing the top speed of the forward motion prototype will give a reference point for setting goals and predictions for future robots. This data can also be used to verify future simulation results, as the motor size, total weight, and the weight of individual components are all known.

The speed test was conducted by measuring the time it took the robot to complete a straight track of known length. This track was 10 feet long and the robot was started 3 feet 4 inches before the track to allow time for the robot to reach full speed. The robot was observed to turn slightly while completing the track, meaning that the actual top speed may be slightly faster than the presented results. The experimental data is presented below. A speed of 3.22 feet per second corresponds to a speed of 2.2 miles per hour.

Trial	Time (s)	Speed (ft/s)
1	2.84	3.52
2	3.15	3.17
3	3.07	3.26
4	3.11	3.22
5	3.41	2.93
Average	-	3.22

Appendix B – Table of Symbols Used in Mathematical Model for Forward Motion

Table II: List of symbols used in derivation and final model.

O_x	x-component of force acting on motor shaft at point *O* (see Figures 8 and 9)
m_m	Mass of internal components (total mass of robot with exception of the outer shell)
a_{cx}	Acceleration in the x direction of the internal components at point *c* (see Figure 9)
O_y	y-component of force acting on motor shaft at point *O* (see Figures 8 and 9)
w_m	Weight force of the internal components
a_{cy}	Acceleration in the y direction of the internal components at point *c* (see Figure 9)
T	Motor torque
J_1	Moment of inertia of the outer shell
$\ddot{\theta}_1$	Angular acceleration of outer shell
r	Distance between points *O* and *c* (see Figure 9)
θ_2	Angular displacement of internal

	components
$\ddot{\theta}_2$	Angular acceleration of internal components
$\vec{R}_c$	Position vector of point *c* relative to x-y coordinate system (see Figures 8 and 9)
$\vec{R}$	Position vector of point *O* relative to x-y coordinate system (see Figures 8 and 9)
$\vec{r}$	Position vector of point *c* relative to point *O* (see Figures 8 and 9)
R	Radius of outer shell
$\dot{\theta}_2$	Angular velocity of internal component

Mathematical Model for reference:

$$J_1\ddot{\theta}_1 - \left[m_m\left(R\ddot{\theta}_1 + r\ddot{\theta}_2\cos\theta_2 - r\dot{\theta}_2{}^2\sin\theta_2\right)\right]r\cos\theta_2 - \left[w_m + m_m\left(r\ddot{\theta}_2\sin\theta_2 + r\dot{\theta}_2{}^2\cos\theta_2\right)\right]r\sin\theta_2 = J_2\ddot{\theta}_2$$

Appendix C- Simulink Model

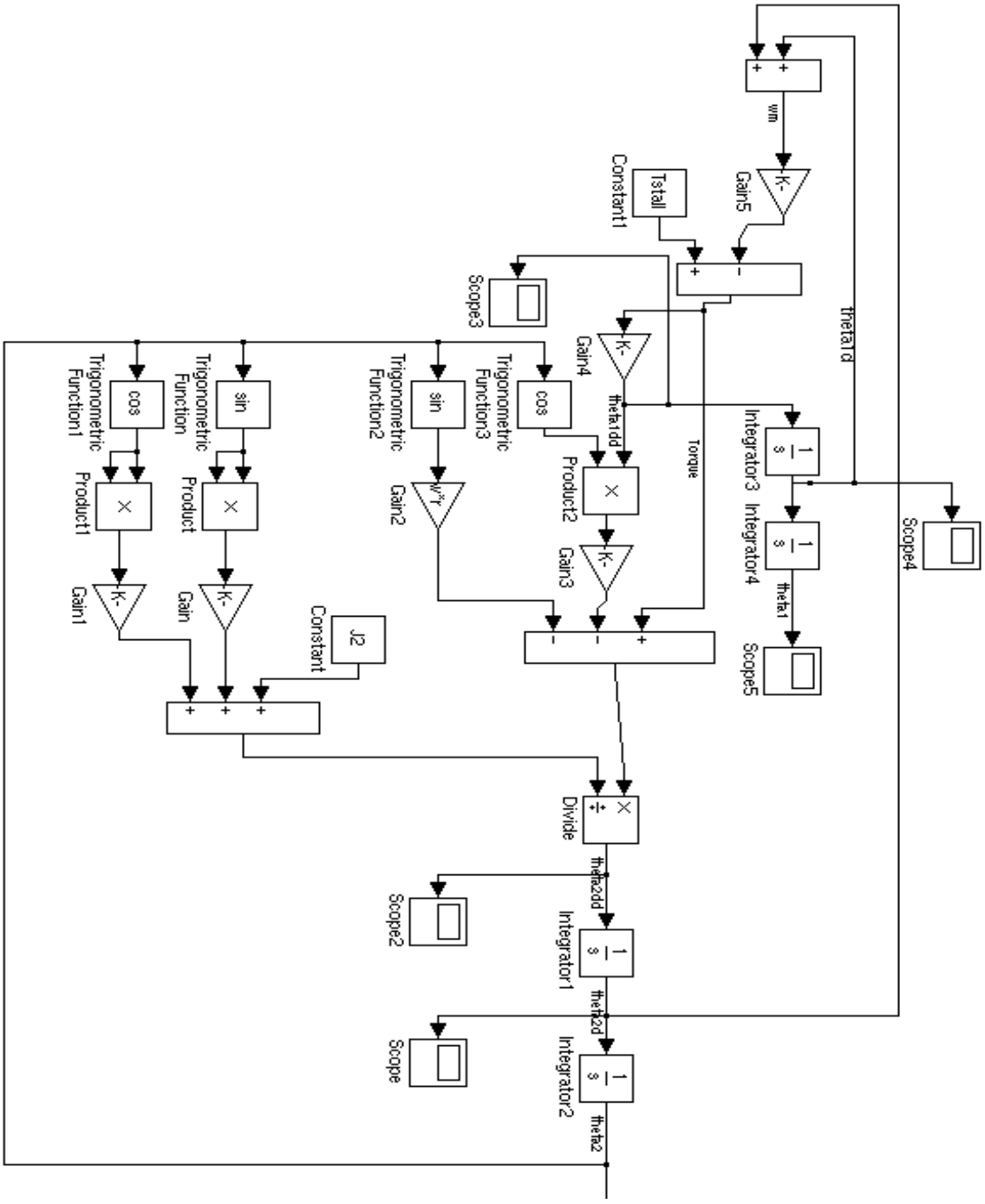

Appendix D – Parameters of Completed Robot

The parameters presented in the table below were all measured or estimated from the finalized robot design. Some parameters, such as motor stall torque and no-load angular velocity, were taken from spec sheets. Other parameters, such as the sphere size and component masses, were actual measurements. The inertial mass moment of the external shell was calculated from the mass and shape of the sphere, while the inertial mass moment of the internal counterweight system was estimated using Solidworks.

Parameter	**Value**
T_{stall}	0.8854 lb ft
ω_{noload}	20.944 s^{-1}
R (radius of sphere)	9 in
Mass of outer shell	5.275 lb
Mass of internal components	
r (distance from driveshaft to center of mass of the internal counterweight)	1.5 in
J_1 (mass moment of external shell)	0.034586126 slug ft^2
J_2 (mass moment of internal counterweight)	

Appendix E - Technical Drawings

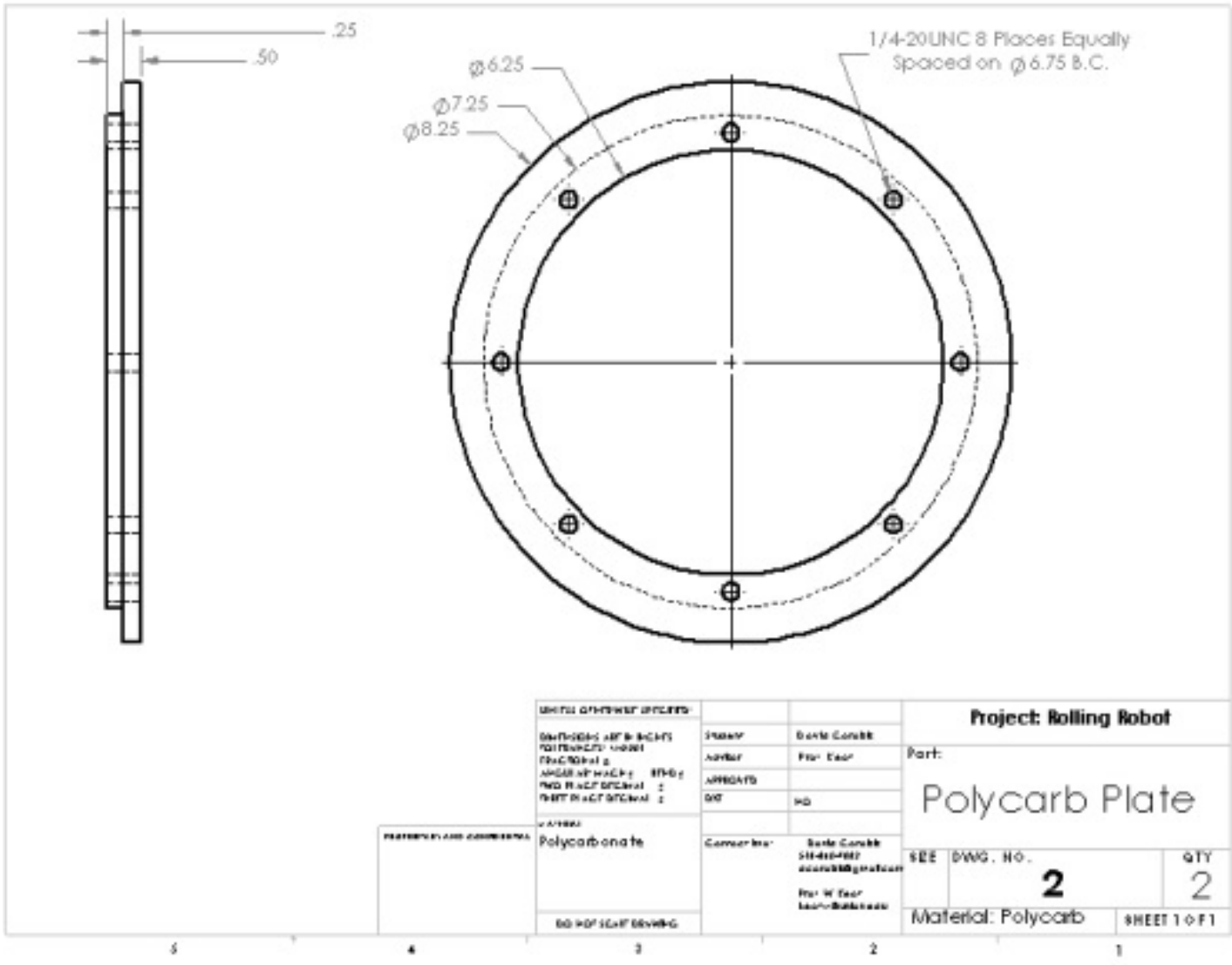
.25
.50
Ø6.25
Ø7.25
Ø8.25
1/4-20UNC 8 Places Equally
Spaced on Ø6.75 B.C.
Project: Rolling Robot
Part:
Polycarb Plate
Polycarbonate
SIZE
DWG. NO.
2
QTY
2
Material: Polycarb
SHEET 1 OF 1

Item No.	Part	QTY.
1	Outer Shell	1
2	Polycarb Plate	2

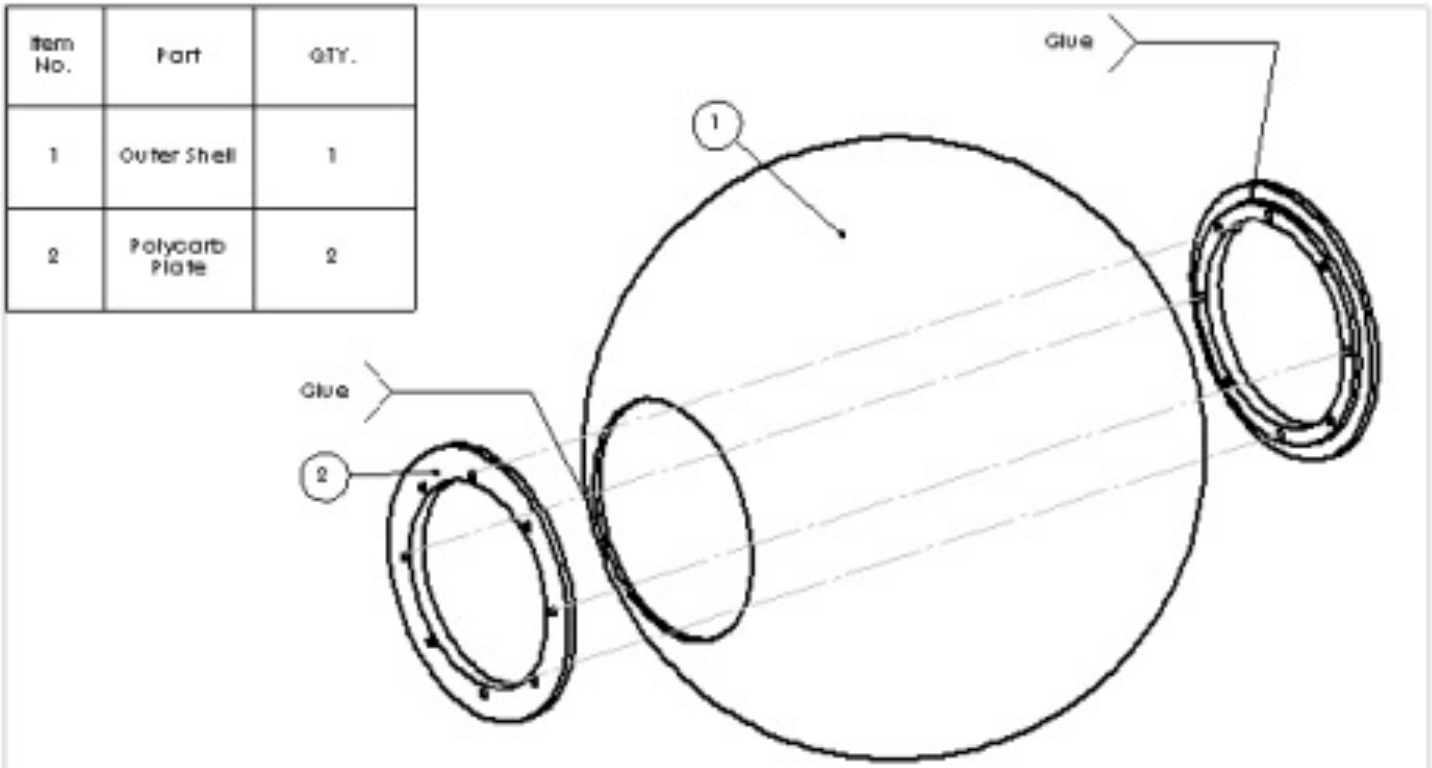

Project: Rolling Robot

Shell Assembly

SIZE | DWG. NO. 3 | QTY. 1

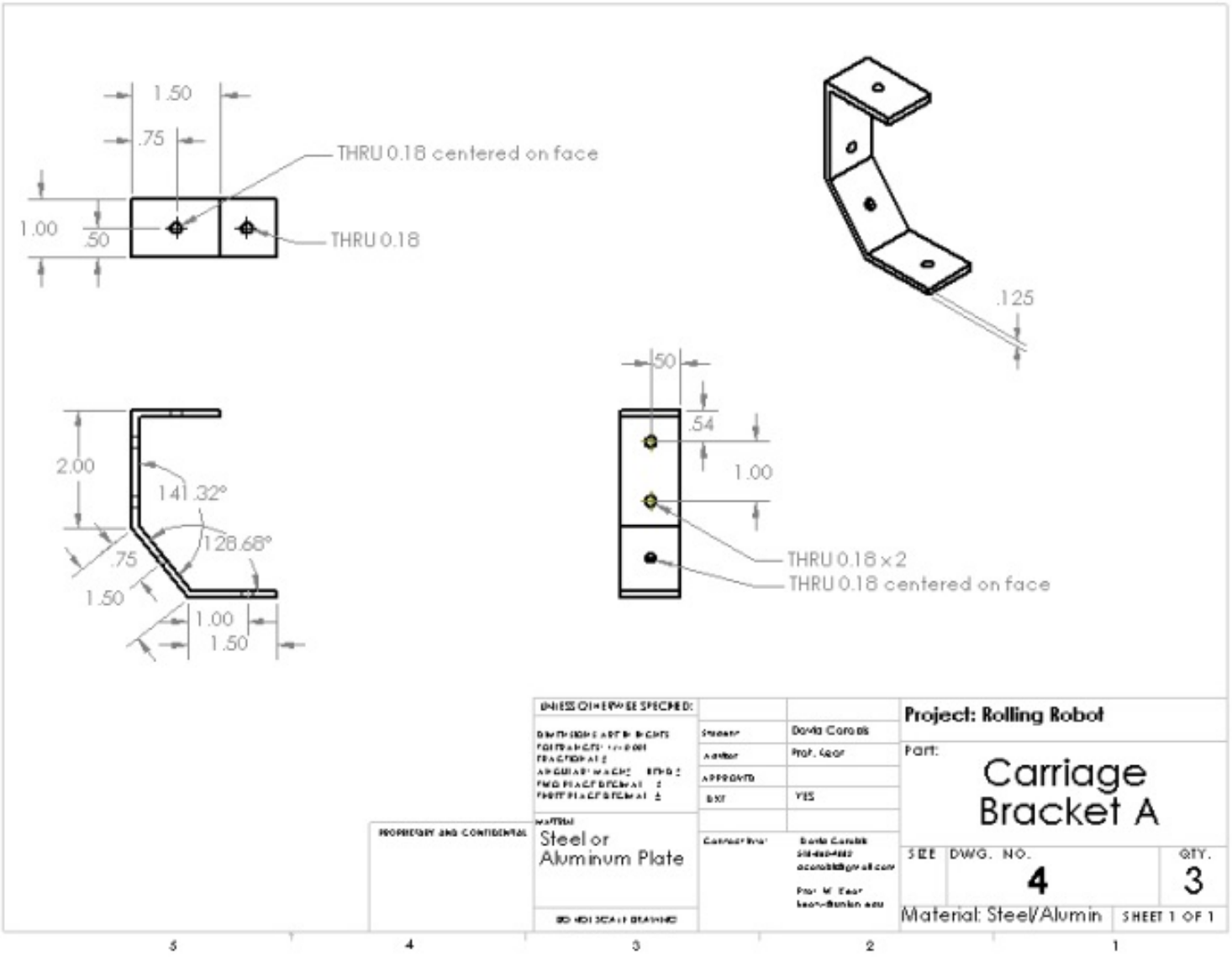
1.50
.75
THRU 0.18 centered on face
1.00
.50
THRU 0.18
.125
.50
.54
1.00
THRU 0.18 x 2
THRU 0.18 centered on face
2.00
141.32°
128.68°
.75
1.50
1.00
1.50
UNLESS OTHERWISE SPECIFIED:
PROPRIETARY AND CONFIDENTIAL
Steel or
Aluminum Plate
Drawn
Dovia Corado
Author
Prof. Geor
APPROVED
DXF
YES
Project: Rolling Robot
Part:
Carriage
Bracket A
SIZE
DWG. NO.
4
QTY.
3
Material: Steel/Alumin
SHEET 1 OF 1

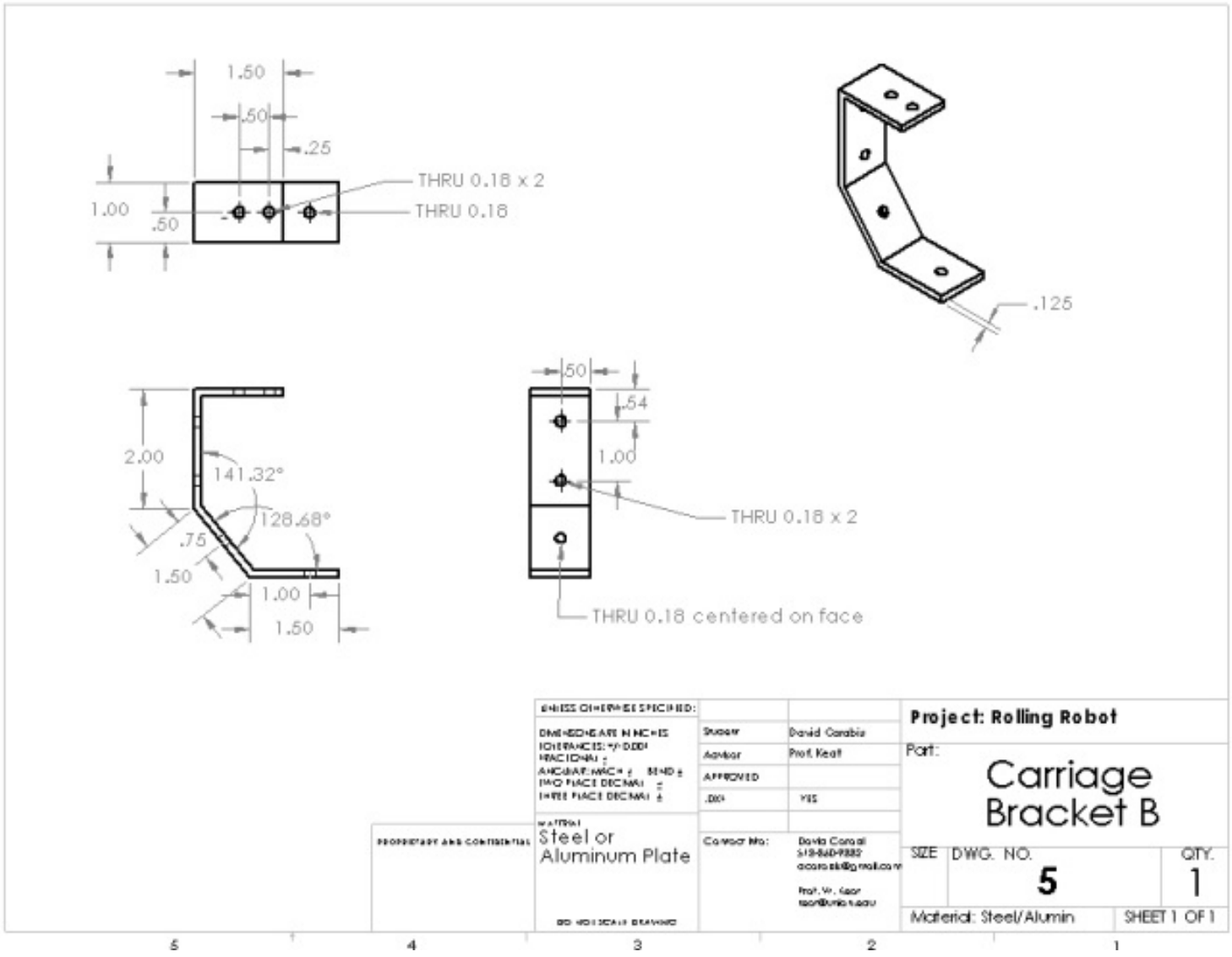
1.50
.50
.25
THRU 0.18 x 2
THRU 0.18
1.00
.50
.125
.50
.54
1.00
2.00
141.32°
128.68°
.75
1.50
1.00
1.50
THRU 0.18 x 2
THRU 0.18 centered on face
UNLESS OTHERWISE SPECIFIED:
DIMENSIONS ARE IN INCHES
TOLERANCES: FRACTIONAL ±
ANGULAR: MACH ± BEND ±
TWO PLACE DECIMAL ±
THREE PLACE DECIMAL ±
MATERIAL
Steel or Aluminum Plate
PROPRIETARY AND CONFIDENTIAL
DO NOT SCALE DRAWING
Drawn
David Corrales
Advisor
Prof. Keat
APPROVED
DATE
YES
Contact Info:
Project: Rolling Robot
Part:
Carriage Bracket B
SIZE
DWG. NO.
5
QTY.
1
Material: Steel/Alumin
SHEET 1 OF 1
5
4
3
2
1

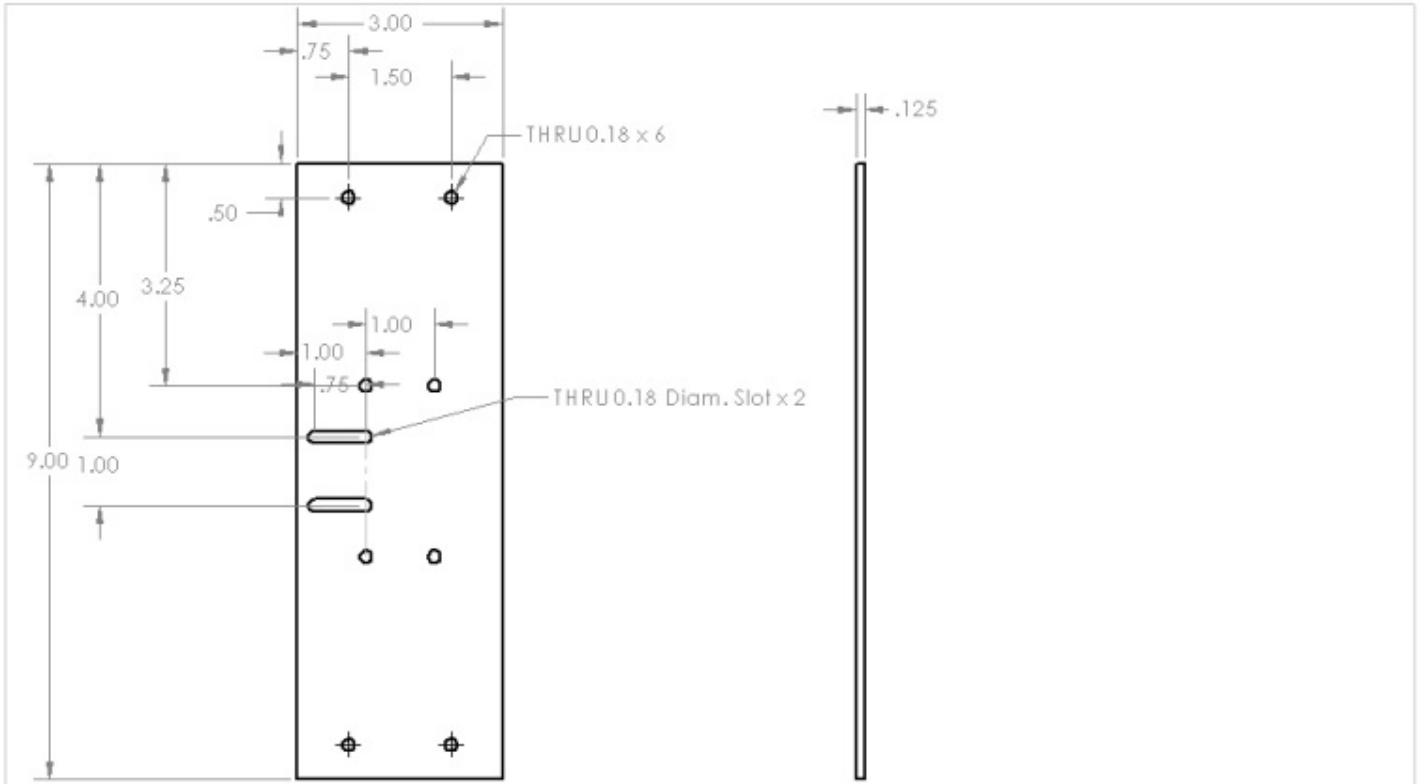
3.00
.75
1.50
.125
THRU 0.18 x 6
.50
4.00
3.25
1.00
1.00
.75
THRU 0.18 Diam. Slot x 2
9.00
1.00
UNLESS OTHERWISE SPECIFIED:
DIMENSIONS ARE IN INCHES
TOLERANCES: +/- 0.001
FRACTIONAL ±
ANGULAR: MACH ± BEND ±
TWO PLACE DECIMAL ±
THREE PLACE DECIMAL ±
MATERIAL
Steel or Aluminum Plate
DO NOT SCALE DRAWING
PROPRIETARY AND CONFIDENTIAL
Student
David Carabis
Advisor
Prof. Keat
APPROVED
DEF
YBI
Contact Info:
David Carabis
518-869-7882
dcarabis@gmail.com
Prof. W. Keat
keatw@union.edu
Project: Rolling Robot
Part:
Under-Carriage
SIZE
DWG. NO.
6
QTY.
1
Material Steel/Aluminum
SHEET 1 OF 1
5
4
3
2
1

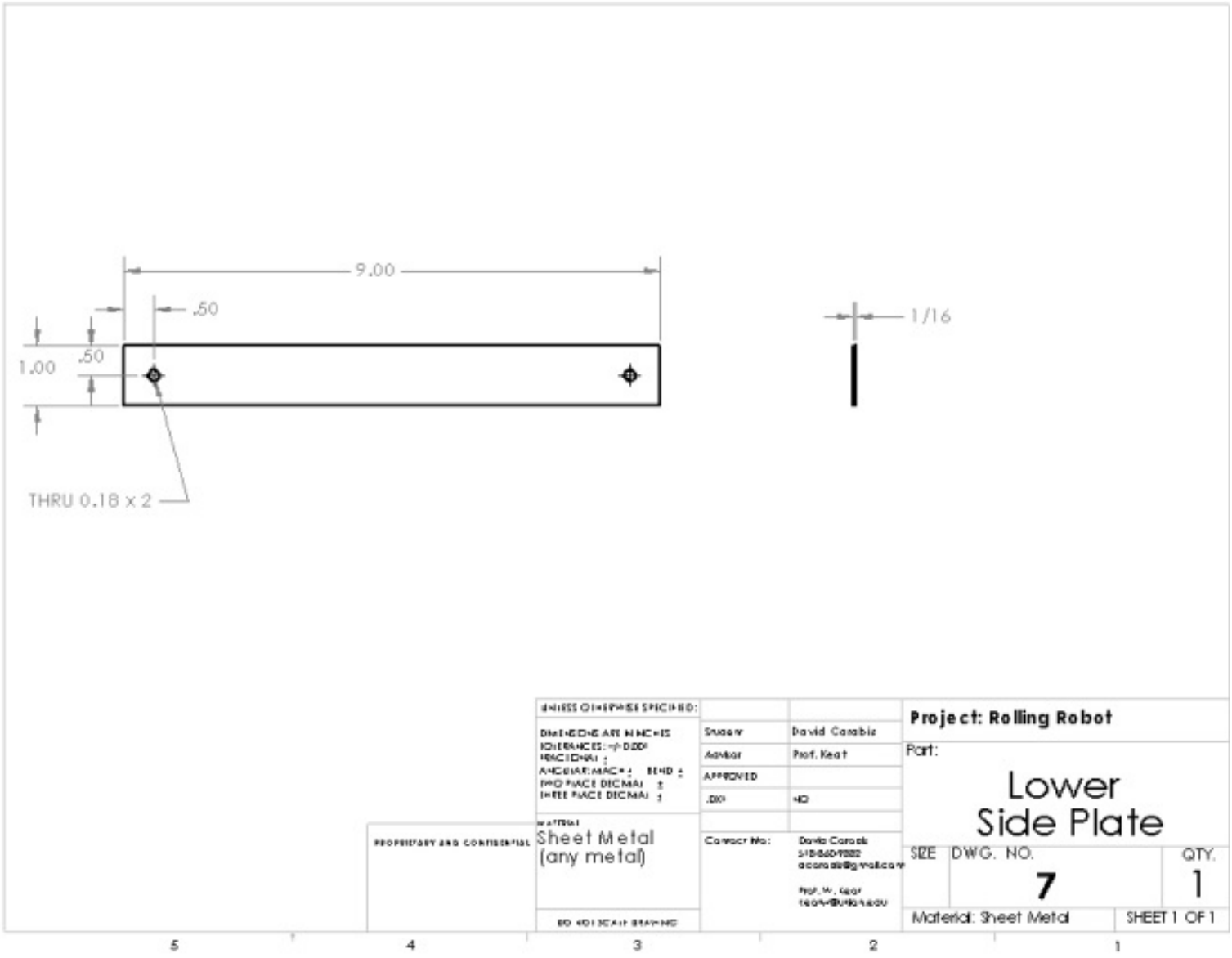
9.00
.50
1.00
.50
THRU 0.18 x 2
1/16
UNLESS OTHERWISE SPECIFIED:
DIMENSIONS ARE IN INCHES
TOLERANCES: FRACTIONAL ±
ANGULAR: MAC ± BEND ±
TWO PLACE DECIMAL ±
THREE PLACE DECIMAL ±
MATERIAL
Sheet Metal (any metal)
NEXT ASSY
USED ON
APPLICATION
DO NOT SCALE DRAWING
PROPRIETARY AND CONFIDENTIAL
Drawn
David Corrado
Check
Prof. Keat
Eng Appr.
MFG Appr.
Comments:
Project: Rolling Robot
Part:
Lower Side Plate
SIZE
DWG. NO.
7
QTY.
1
Material: Sheet Metal
SHEET 1 OF 1
5
4
3
2
1

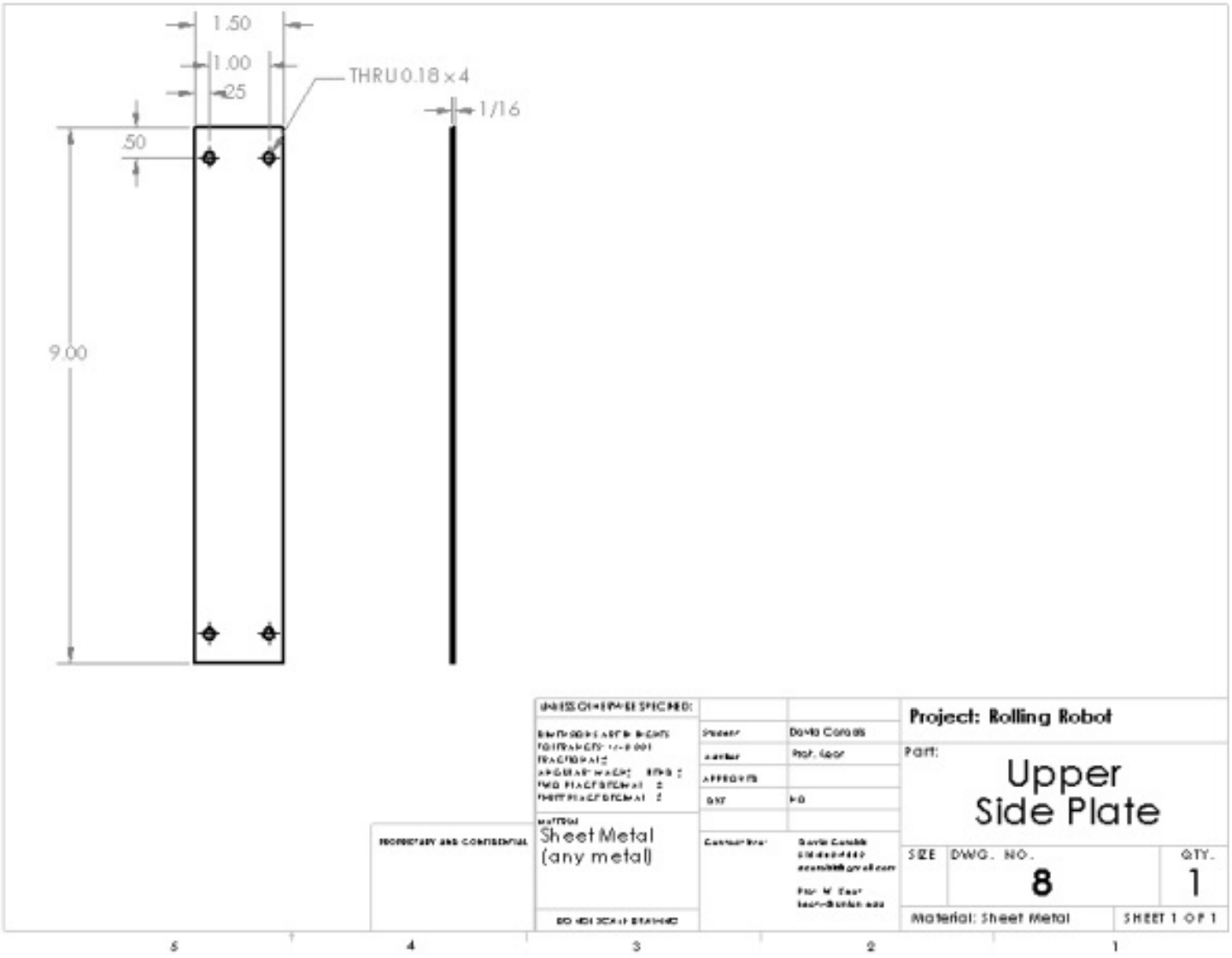
1.50
1.00
.25
THRU 0.18 x 4
1/16
.50
9.00
UNLESS OTHERWISE SPECIFIED:
PROPRIETARY AND CONFIDENTIAL
Sheet Metal
(any metal)
DO NOT SCALE DRAWING
Student
David Corrales
Number
Prof. Goor
APPROVED
DATE
NO
Project: Rolling Robot
PART:
Upper
Side Plate
SIZE
DWG. NO.
8
QTY.
1
Material: Sheet Metal
SHEET 1 OF 1
5
4
3
2
1

ITEM NO.	PART	QTY.
4	Carriage Bracket A	3
5	Carriage Bracket B	1
6	Undercarraige Plate	1
7	Lower Side Plate	1
8	Upper Side Plate	1
A	8-32 Machine Screw	10
B	8-32 Nut	10

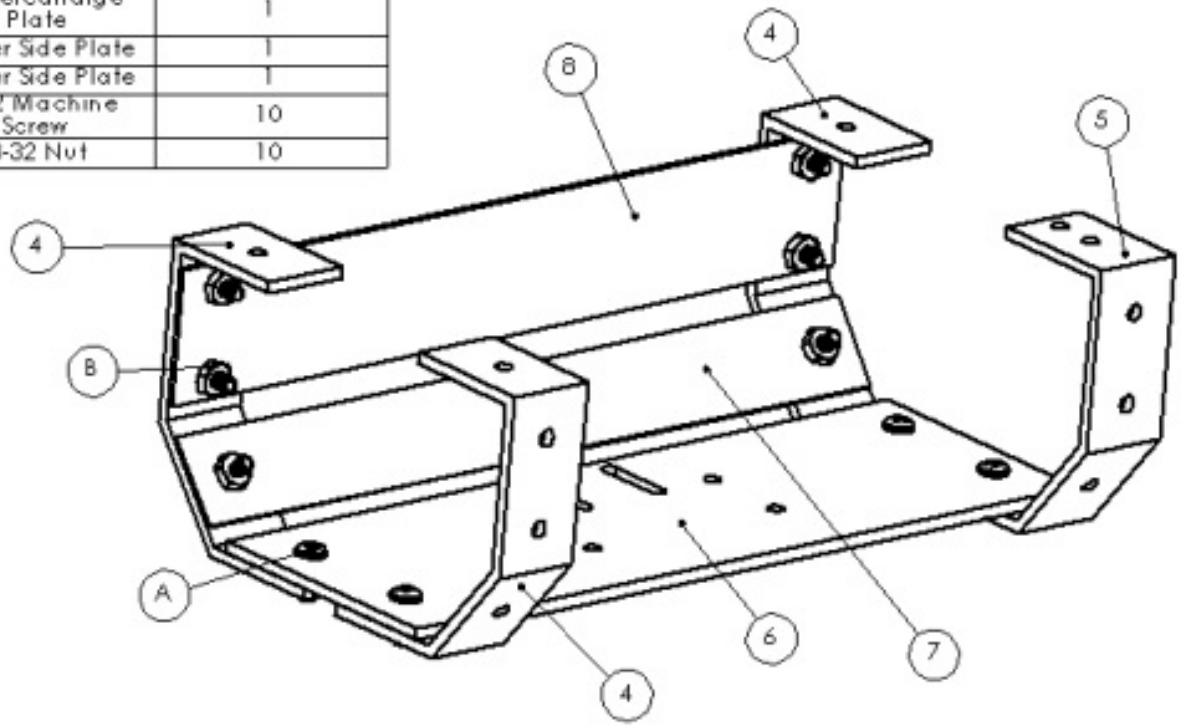

UNLESS OTHERWISE SPECIFIED:
DIMENSIONS ARE IN INCHES
TOLERANCES: +/- 0.001
FRACTIONAL ±
ANGULAR: MACH ± BEND ±
TWO PLACE DECIMAL ±
THREE PLACE DECIMAL ±
MATERIAL
PROPRIETARY AND CONFIDENTIAL
DO NOT SCALE DRAWING

Drawn	Dovia Corcelli	
Checked	Prof. Gear	
APPROVED		
DO	NO	
Contact Info:	Dovia Corcelli 315-560-9282 dcorcelli@gmail.com Prof. W. Gear wgear@union.edu	

Project: Rolling Robot

PART:
Undercarriage Assembly

SIZE	DWG. NO.	QTY.
	9	1

SHEET 1 OF 1

5 4 3 2 1

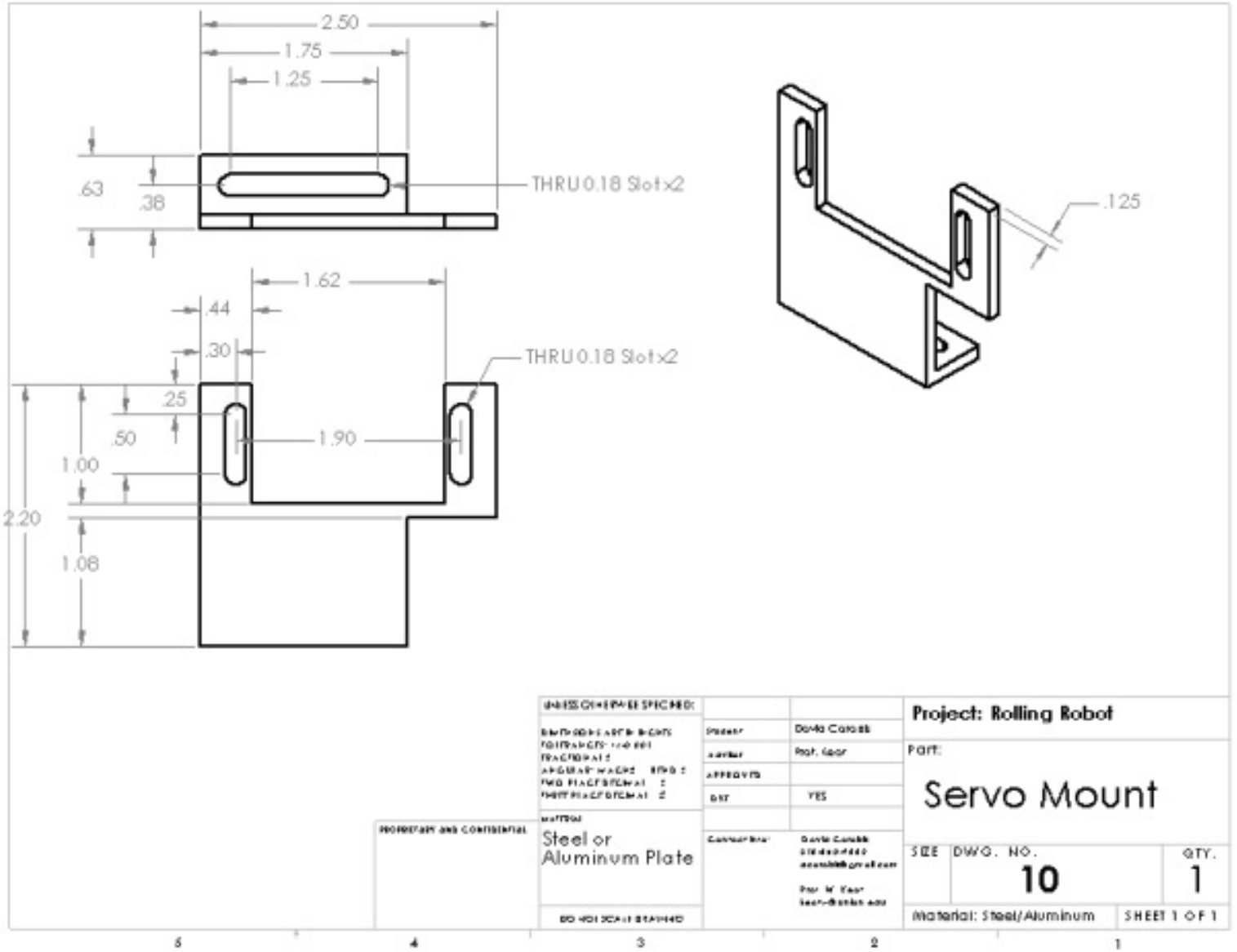
2.50
1.75
1.25
.63
.38
THRU 0.18 Slot x2
1.62
.44
.30
THRU 0.18 Slot x2
.25
.50
1.90
1.00
2.20
1.08
.125
Project: Rolling Robot
Part:
Servo Mount
Steel or
Aluminum Plate
SIZE
DWG. NO.
10
QTY.
1
Material: Steel/Aluminum
SHEET 1 OF 1

Item No.	Part	QTY.
10	Servo Mount	1
A	8-32 Machine Screw	4
B	8-32 Nut	4
C	Futaba Servo	1
D	Plastic Servo Gear	1

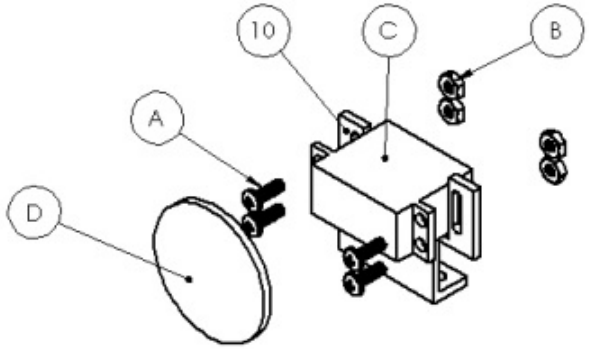

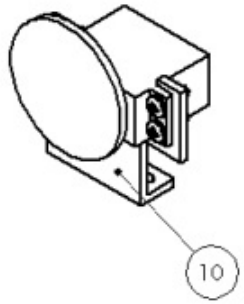

UNLESS OTHERWISE SPECIFIED:

DIMENSIONS ARE IN INCHES
TOLERANCES: +/- 0.001
FRACTIONAL ±
ANGULAR: MACH ± BEND ±
TWO PLACE DECIMAL ±
THREE PLACE DECIMAL ±

MATERIAL

PROPRIETARY AND CONFIDENTIAL

DO NOT SCALE DRAWING

Student	David Carabis
Advisor	Prof. Keat
APPROVED	
.DXF	NO

Contact Info: David Carabis
518-860-9882
dcarabis@gmail.com

Prof. W. Keat
keatw@union.edu

Project: Rolling Robot

Part:

Servo Assembl

SIZE | DWG. NO. 11

SHEET 1

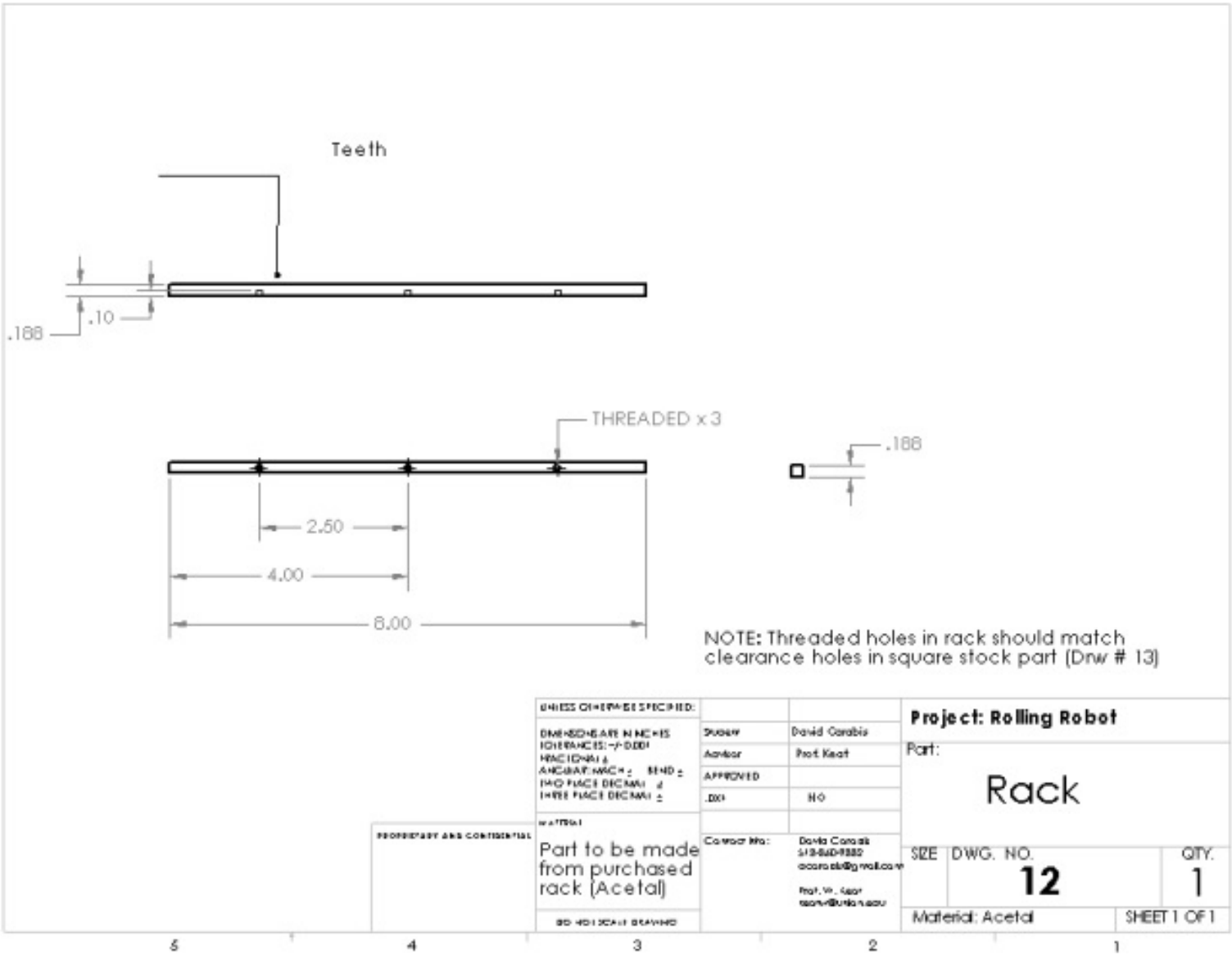
Teeth
.188
.10
THREADED x 3
.188
2.50
4.00
8.00
NOTE: Threaded holes in rack should match clearance holes in square stock part (Drw # 13)
UNLESS OTHERWISE SPECIFIED:
DIMENSIONS ARE IN INCHES
TOLERANCES: FRACTIONAL ±
ANGULAR: MACH ± BEND ±
TWO PLACE DECIMAL ±
THREE PLACE DECIMAL ±
MATERIAL
Part to be made from purchased rack (Acetal)
NEXT ASSY
PROPRIETARY AND CONFIDENTIAL
Student
David Corrado
Advisor
Prof. Kaur
APPROVED
DWG
NO
Company Info:
David Corrado
Prof. M. Kaur
Project: Rolling Robot
Part:
Rack
SIZE
DWG. NO.
12
QTY.
1
Material: Acetal
SHEET 1 OF 1
5
4
3
2
1

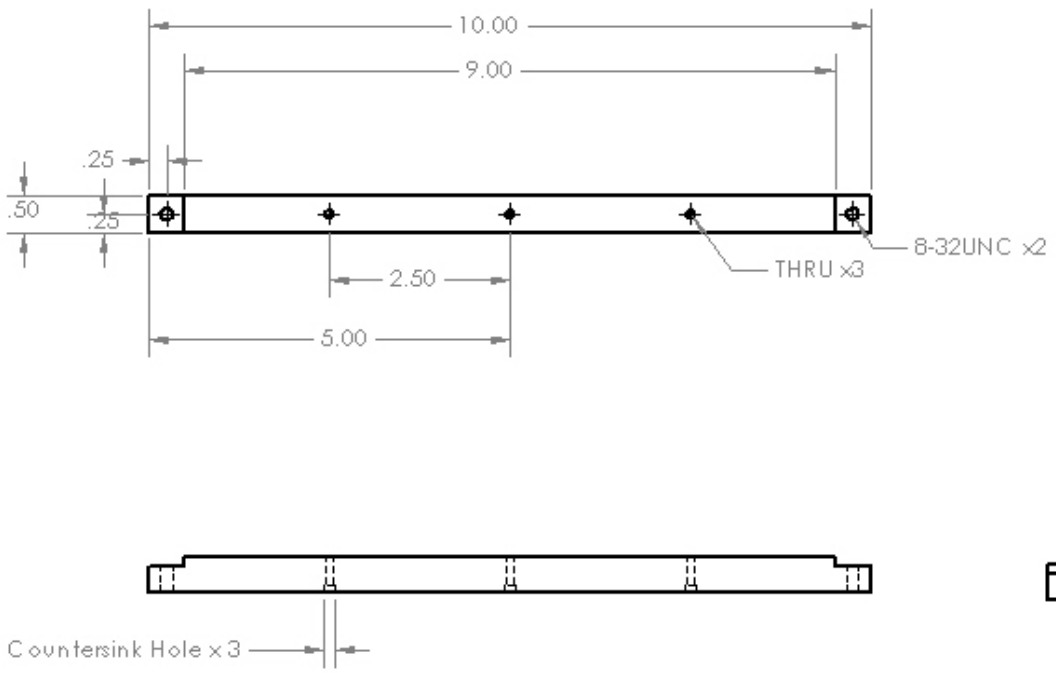

NOTE: THRU holes shound match
THREADED holes on rack part (Drw # 12)

UNLESS OTHERWISE SPECIFIED:			Project: Rolling Robot
DIMENSIONS ARE IN INCHES TOLERANCES: +/- 0.001 FRACTIONAL ± ANGULAR: MACH ± BEND ± TWO PLACE DECIMAL ± THREE PLACE DECIMAL ±	Student	Davia Corrals	Part: Square Stock
	Advisor	Prof. Gear	
	APPROVED		
	.DXF	NO	
MATERIAL PVC	Contact Info:	Davia Corrals 518-860-9882 dcorrals@gmail.com Prof. W. Gear gearw@union.edu	SIZE: — DWG. NO.: 13 — QTY.: 1
PROPRIETARY AND CONFIDENTIAL			Material: PVC — SHEET 1 OF 1
DO NOT SCALE DRAWING			

5 4 3 2 1

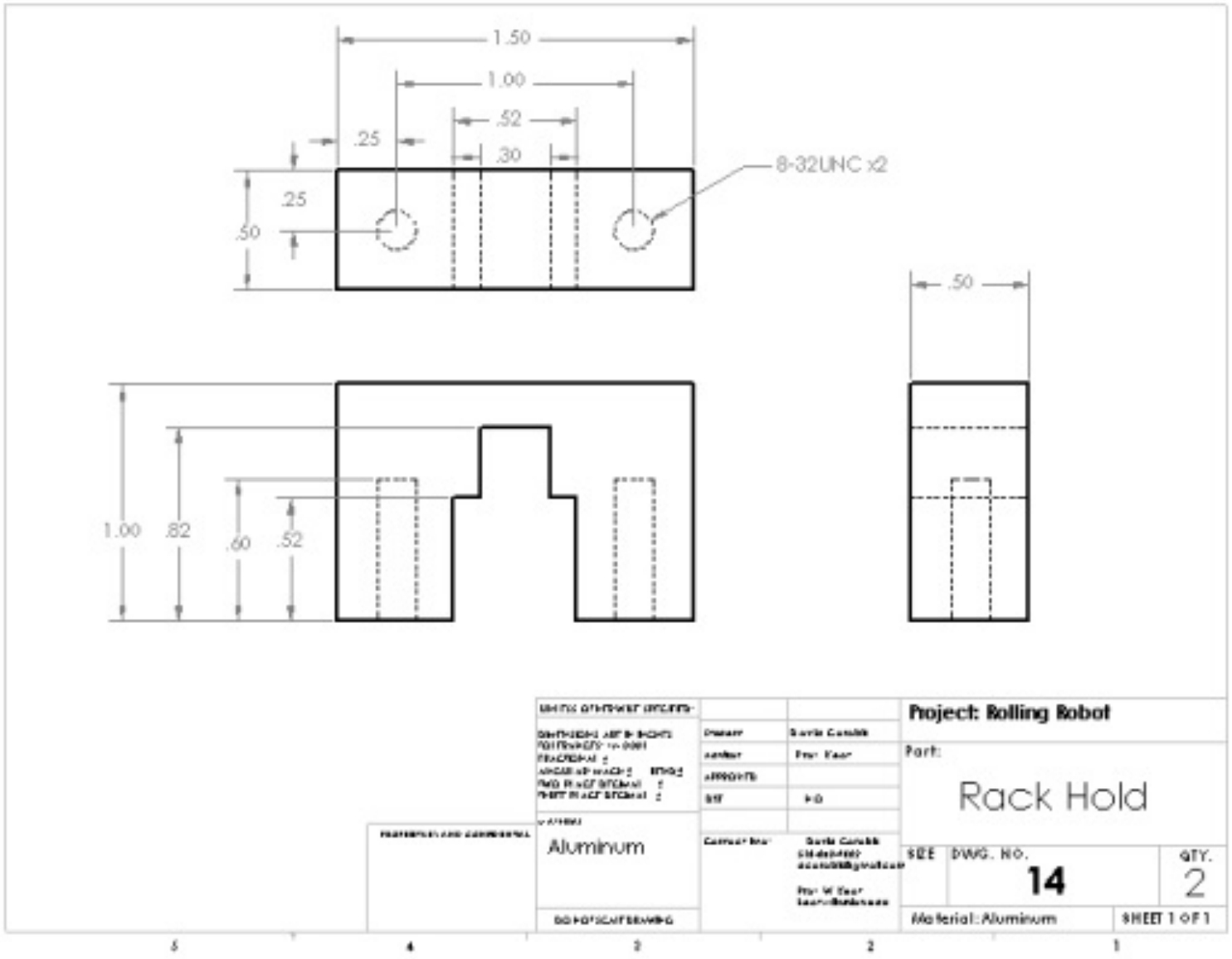
1.50
1.00
.52
.30
.25
8-32UNC x2
.25
.50
.50
1.00
.82
.60
.52
Aluminum
Project: Rolling Robot
Part:
Rack Hold
SIZE
DWG. NO.
14
QTY.
2
Material: Aluminum
SHEET 1 OF 1

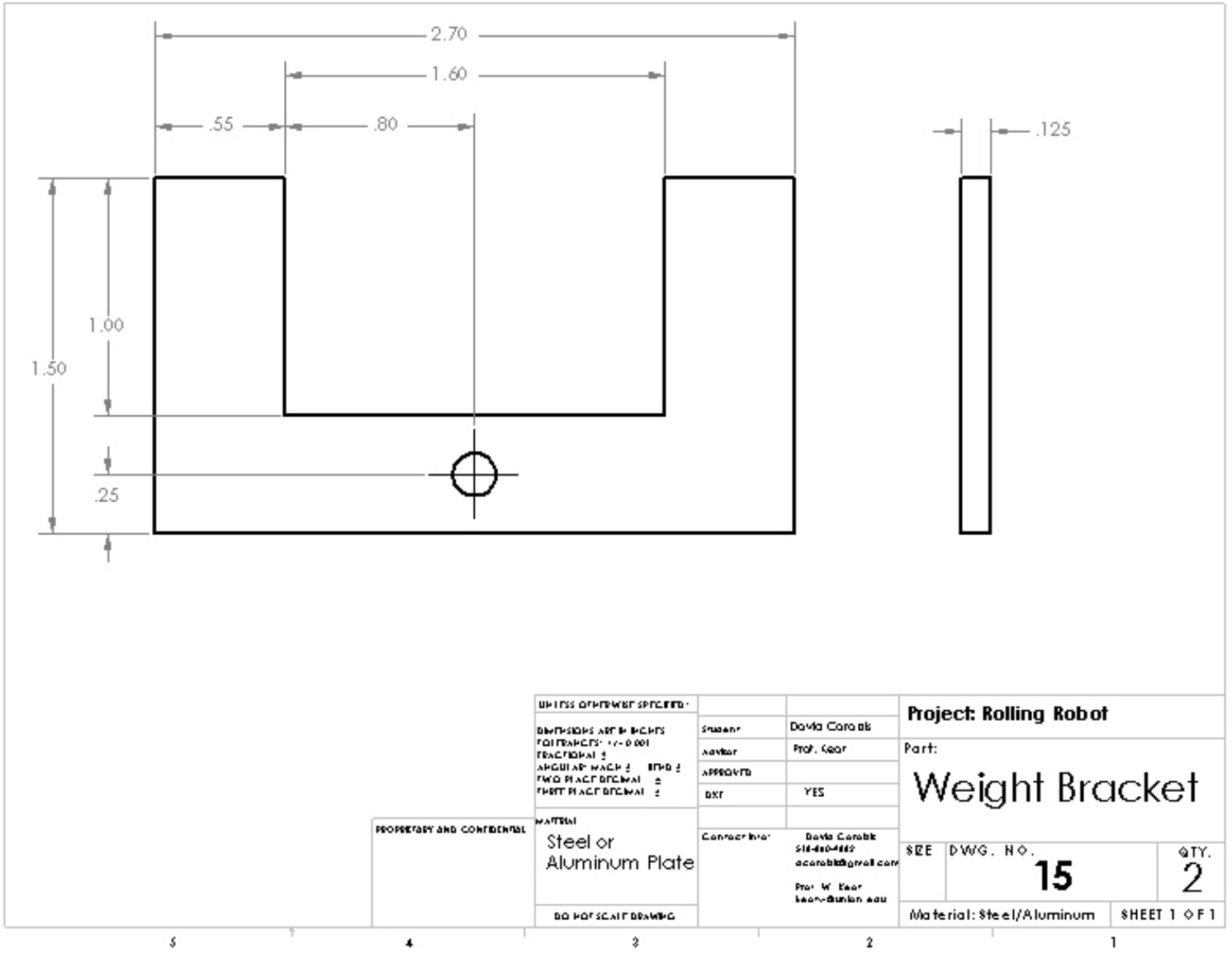
2.70
1.60
.55
.80
.125
1.00
1.50
.25
UNLESS OTHERWISE SPECIFIED:
DIMENSIONS ARE IN INCHES
TOLERANCES: FRACTIONAL ±
ANGULAR: MACH ± BEND ±
TWO PLACE DECIMAL ±
THREE PLACE DECIMAL ±
MATERIAL
Steel or Aluminum Plate
DO NOT SCALE DRAWING
PROPRIETARY AND CONFIDENTIAL
Student
Davis Carabb
Author
Prof. Geer
APPROVED
DXF
YES
Contact Info:
Davis Carabb
Prof. W. Geer
Project: Rolling Robot
Part:
Weight Bracket
SIZE
DWG. NO.
15
QTY.
2
Material: Steel/Aluminum
SHEET 1 OF 1

Item No.	Part	QTY.
9	Under Carriage Assembly	1
11	Servo Assembly	1
12	Rack	1
13	Square Stock	1
14	Rack Hold	2
15	Weight Bracket	2
A	8-32 Machine Screw	8
B	8-32 Nut	2

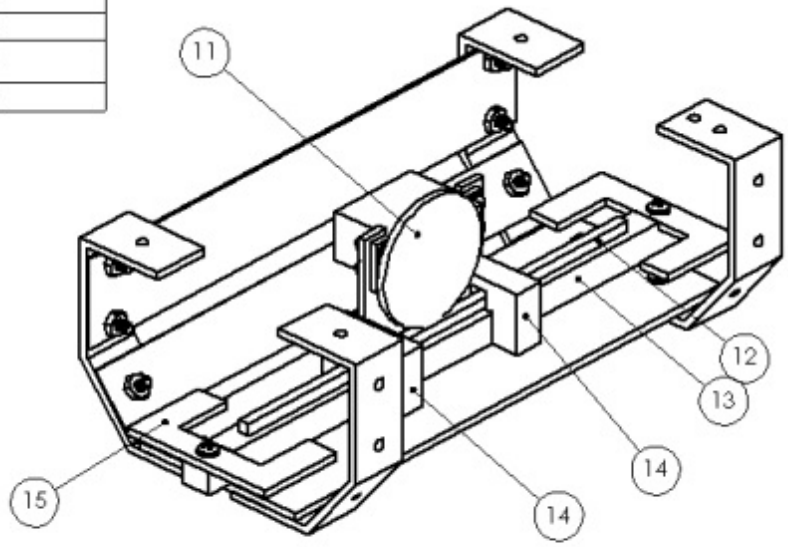

UNLESS OTHERWISE SPECIFIED:

DIMENSIONS ARE IN INCHES
TOLERANCES: +/- 0.001
FRACTIONAL ±
ANGULAR: MACH ± BEND ±
TWO PLACE DECIMAL ±
THREE PLACE DECIMAL ±

MATERIAL

DO NOT SCALE DRAWING

PROPRIETARY AND CONFIDENTIAL

Student	David Corrado
Advisor	Prof. Keat
APPROVED	
.DXF	NO

Contact Info: David Corrado 518-860-9882 dcorrado@gmail.com
Prof. W. Keat rearw@union.edu

Project: Rolling Robot

Part: Turning Mech Assembly

SIZE	DWG. NO.	QTY.
	16	1

SHEET 1 OF 1

5 4 3 2 1

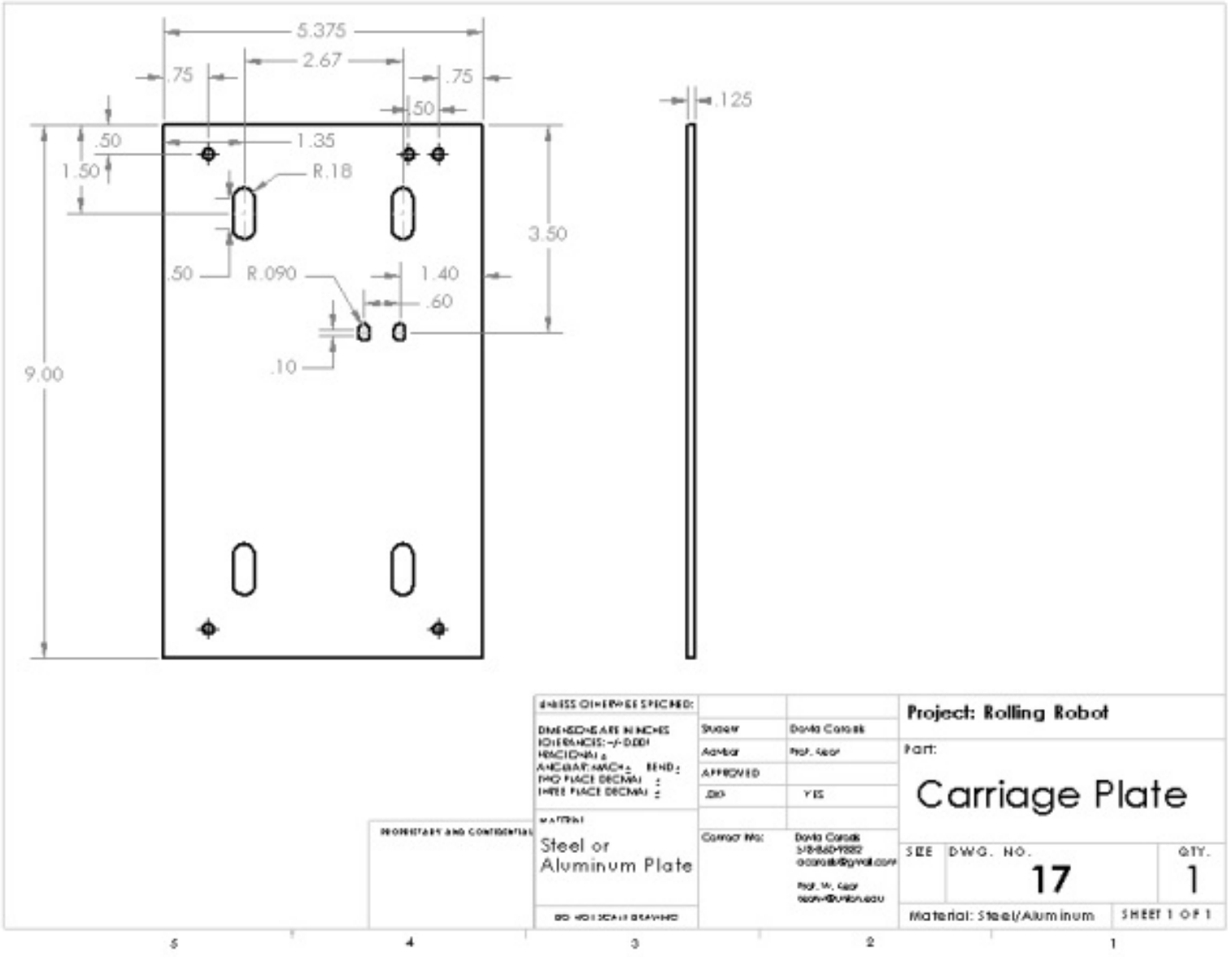
5.375
2.67
.75
.75
.50
.125
.50
1.35
1.50
R.18
3.50
.50
R.090
1.40
.60
.10
9.00
UNLESS OTHERWISE SPECIFIED:
DIMENSIONS ARE IN INCHES
TOLERANCES: +/- 0.001
FRACTIONAL ±
ANGULAR: MACH ± BEND ±
TWO PLACE DECIMAL ±
THREE PLACE DECIMAL ±
MATERIAL
Steel or Aluminum Plate
DO NOT SCALE DRAWING
PROPRIETARY AND CONFIDENTIAL
Drawn
Dovia Corado
Checked
Prof. Yabor
APPROVED
DATE
YES
Company Name
Dovia Corado
Prof. W. Yabor
Project: Rolling Robot
PART:
Carriage Plate
SIZE
DWG. NO.
17
QTY.
1
Material: Steel/Aluminum
SHEET 1 OF 1
5
4
3
2
1

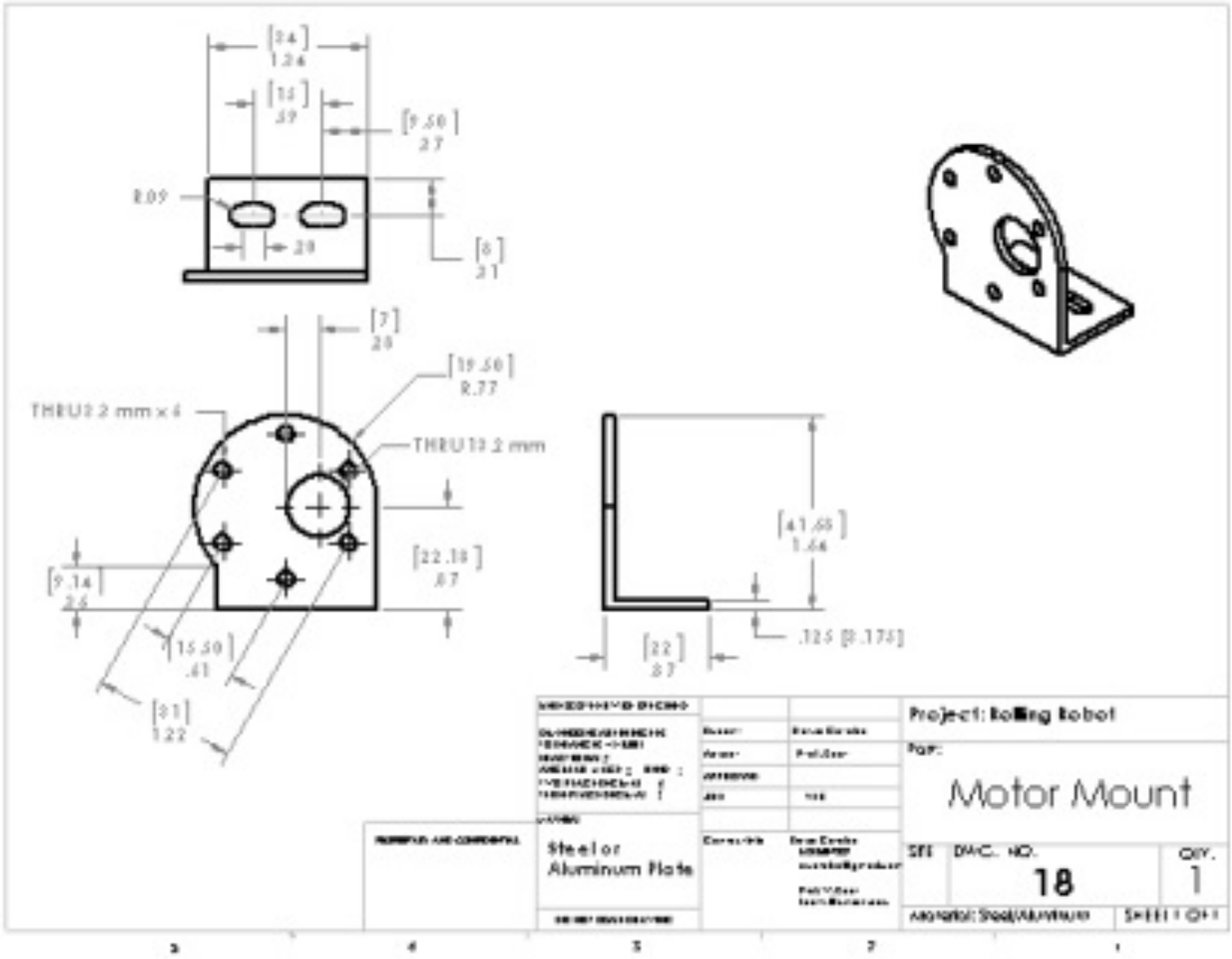
[24]
1.24
[15]
.59
[9.50]
.37
8.09
20
[6]
.31
[7]
.28
[19.50]
R.77
THRU 3.2 mm x 4
THRU 13.2 mm
[22.18]
.87
[9.14]
.36
[15.50]
.61
[31]
1.22
[41.65]
1.64
.125 [3.175]
[22]
.87
Project: Rolling Robot
Motor Mount
Steel or
Aluminum Plate
SIZE
DWG. NO.
18
QTY.
1

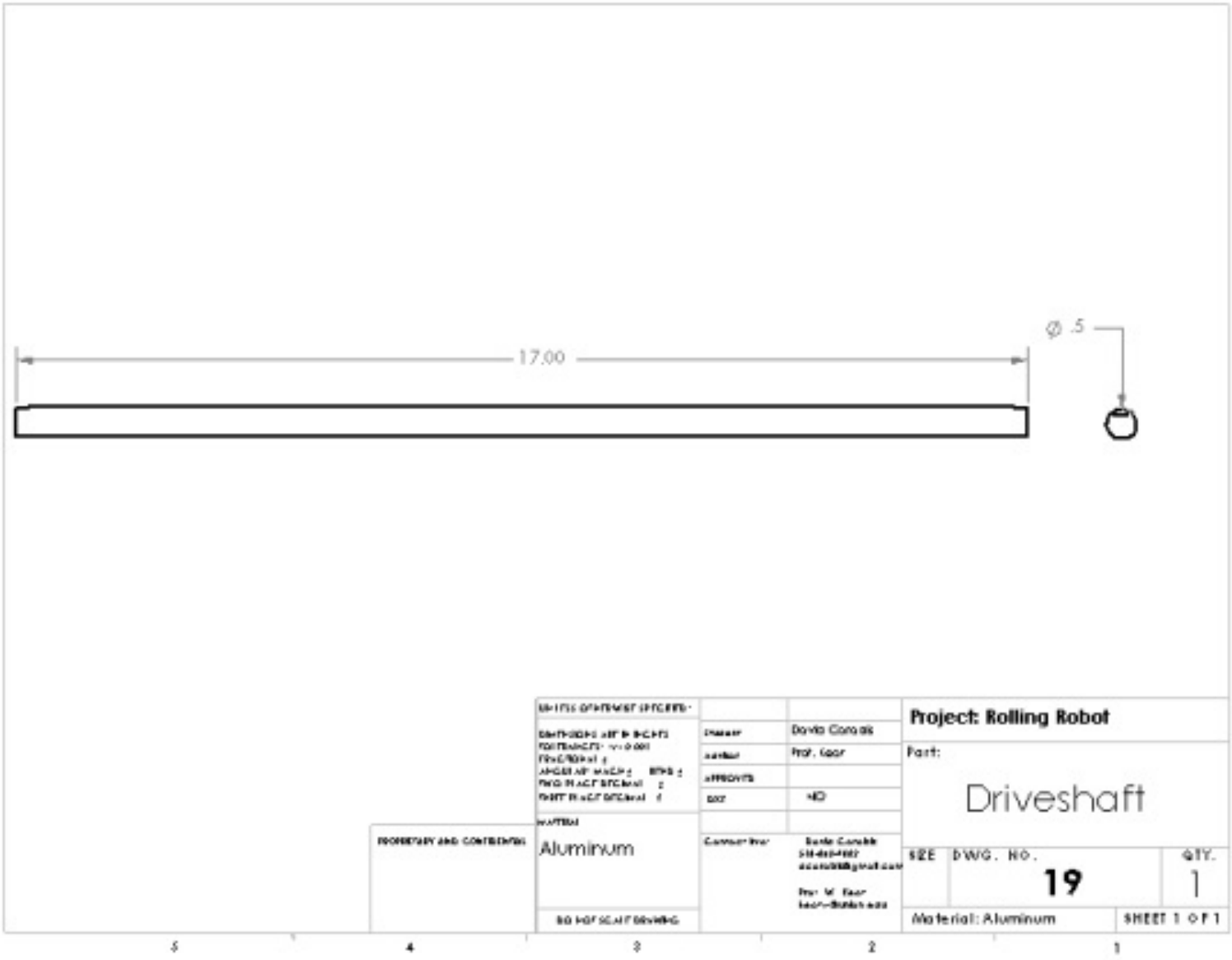
17.00
Ø .5
Project: Rolling Robot
Part:
Driveshaft
Aluminum
Material: Aluminum
SIZE
DWG. NO.
19
QTY.
1
SHEET 1 OF 1

Item No.	Part	QTY.
17	Carriage Plate	1
18	Motor Mount	1
19	Driveshaft	1
A	8-32 Machine Screw	2
B	8-32 Nut	2
E	1/4-20 Machine Screw	4
F	1/4-20 Nut	4
G	3mm Machine Screw	6
H	Ball Bearing	2
I	Gear (Large)	1
J	Gear (Small)	1
K	Motor	1

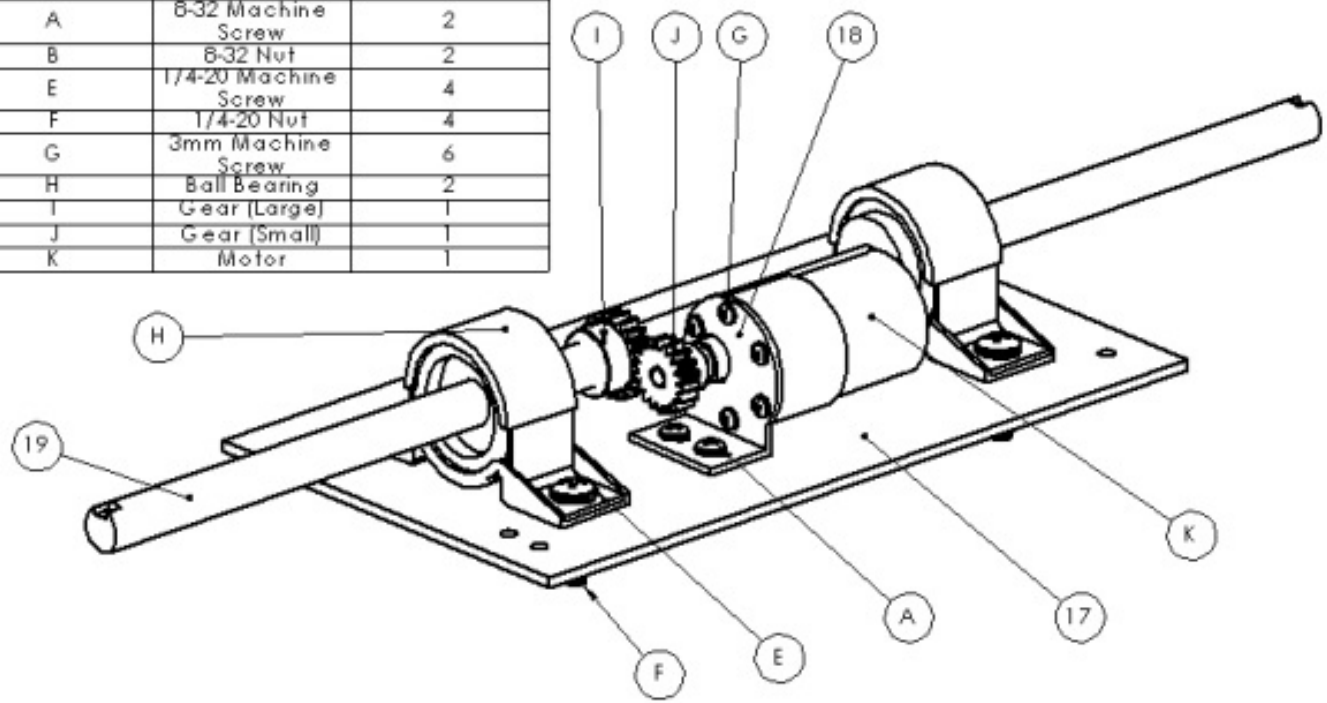

UNLESS OTHERWISE SPECIFIED:
DIMENSIONS ARE IN INCHES
TOLERANCES: FRACTIONAL ±
ANGULAR: MACH ± BEND ±
TWO PLACE DECIMAL ±
THREE PLACE DECIMAL ±
MATERIAL
PROPRIETARY AND CONFIDENTIAL
DO NOT SCALE DRAWING

Student	David Carob
Advisor	Prof. Lear
APPROVED	
.001	NO
Contact Info:	David Carob 518-860-9882 dcarob86@rpi.edu Prof. M. Lear learm@rpi.edu

Project: Rolling Robot

PART:

Driveshaft Assembly

SIZE	DWG. NO.	QTY.
	20	1

SHEET 1 OF 1

5 4 3 2 1

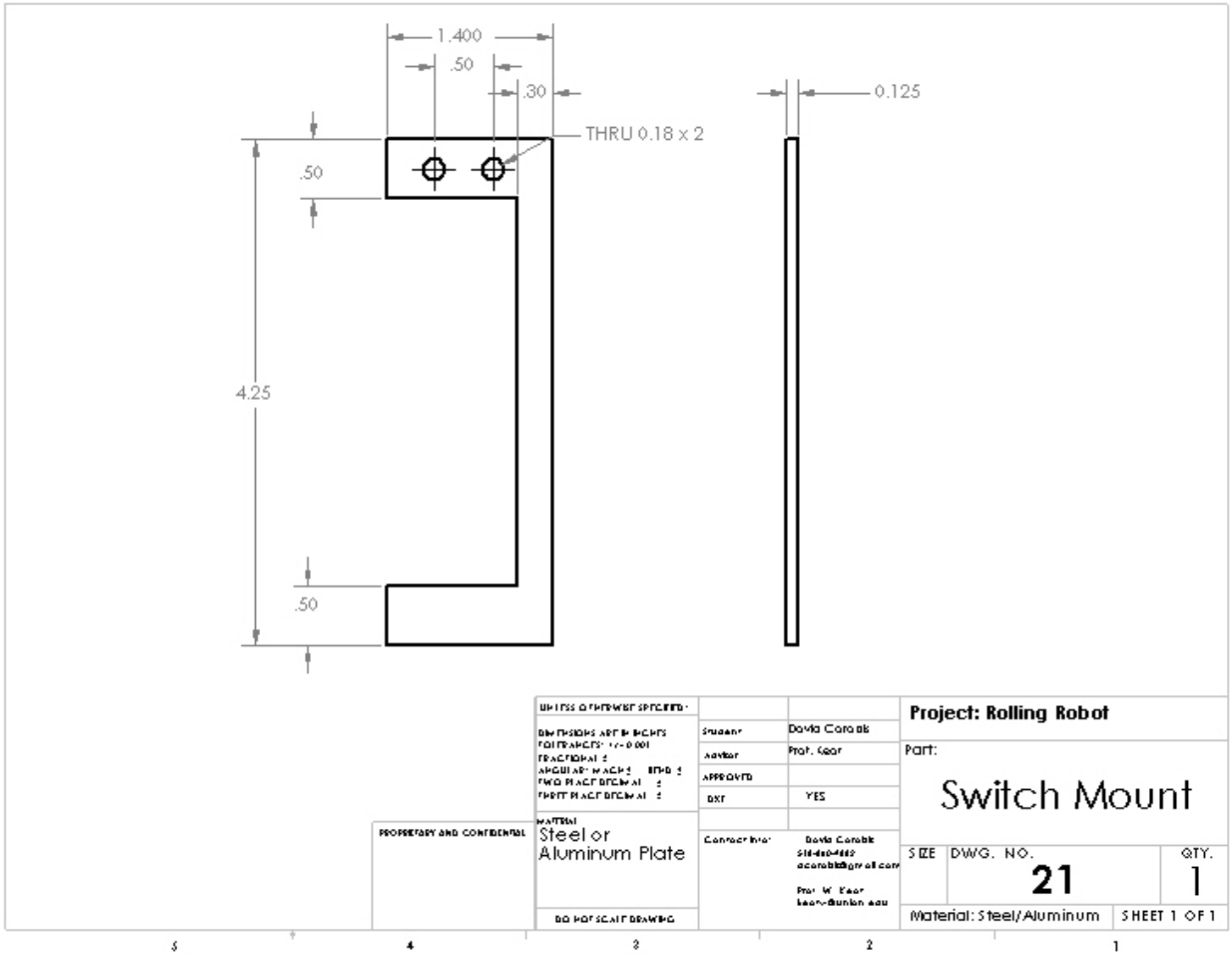
1.400
.50
.30
0.125
THRU 0.18 x 2
.50
4.25
.50
UNLESS OTHERWISE SPECIFIED:
DIMENSIONS ARE IN INCHES
TOLERANCES: +/- 0.001
FRACTIONAL ±
ANGULAR: MACH ± BEND ±
TWO PLACE DECIMAL ±
THREE PLACE DECIMAL ±
MATERIAL
Steel or
Aluminum Plate
DO NOT SCALE DRAWING
PROPRIETARY AND CONFIDENTIAL
Student
Davis Corrado
Advisor
Prof. Geer
APPROVED
DXF
YES
Contact Info:
Davis Corrado
Prof. W. Geer
Project: Rolling Robot
Part:
Switch Mount
SIZE
DWG. NO.
21
QTY.
1
Material: Steel/Aluminum
SHEET 1 OF 1
5
4
3
2
1

ITEM NO.	Part	QTY.
16	Turning Mech Assembly	1
20	Driveshaft Assembly	1
21	Switch Mount	1
22	Driveshaft Plate	2
A	8-32 Machine Screw	5
B	8-32 Nut	5

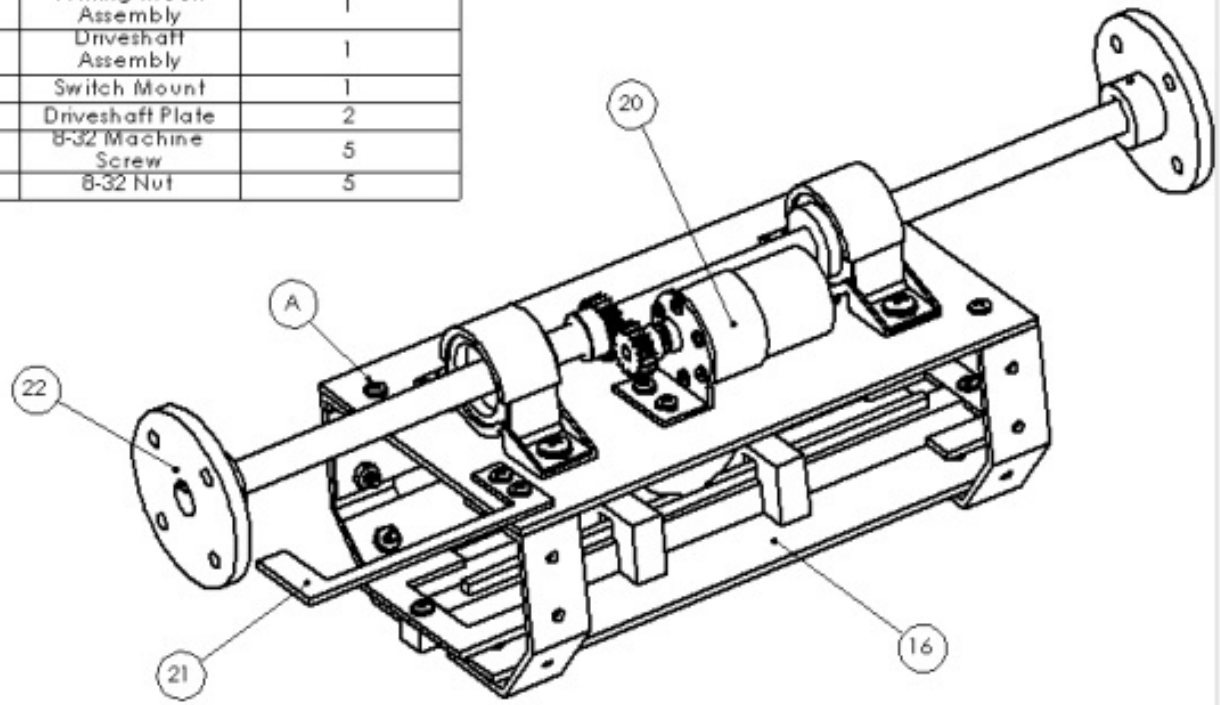

UNLESS OTHERWISE SPECIFIED:
DIMENSIONS ARE IN INCHES
TOLERANCES: +/- 0.001
FRACTIONAL ±
ANGULAR: MACH ± BEND ±
TWO PLACE DECIMAL ±
THREE PLACE DECIMAL ±
MATERIAL
PROPRIETARY AND CONFIDENTIAL
NEXT ASSY
DO NOT SCALE DRAWING

Student	David Corcoran	
Advisor	Prof. Geor	
APPROVED		
DWG	NO	
Contact Info:	David Corcoran 518-860-9882 dcoran.ski@gmail.com Prof. Geor geom@union.edu	

Project: Rolling Robot

Part: Internal Components Assembly

SIZE	DWG. NO.	QTY.
	23	1

SHEET 1 OF 1

8 4 3 2 1

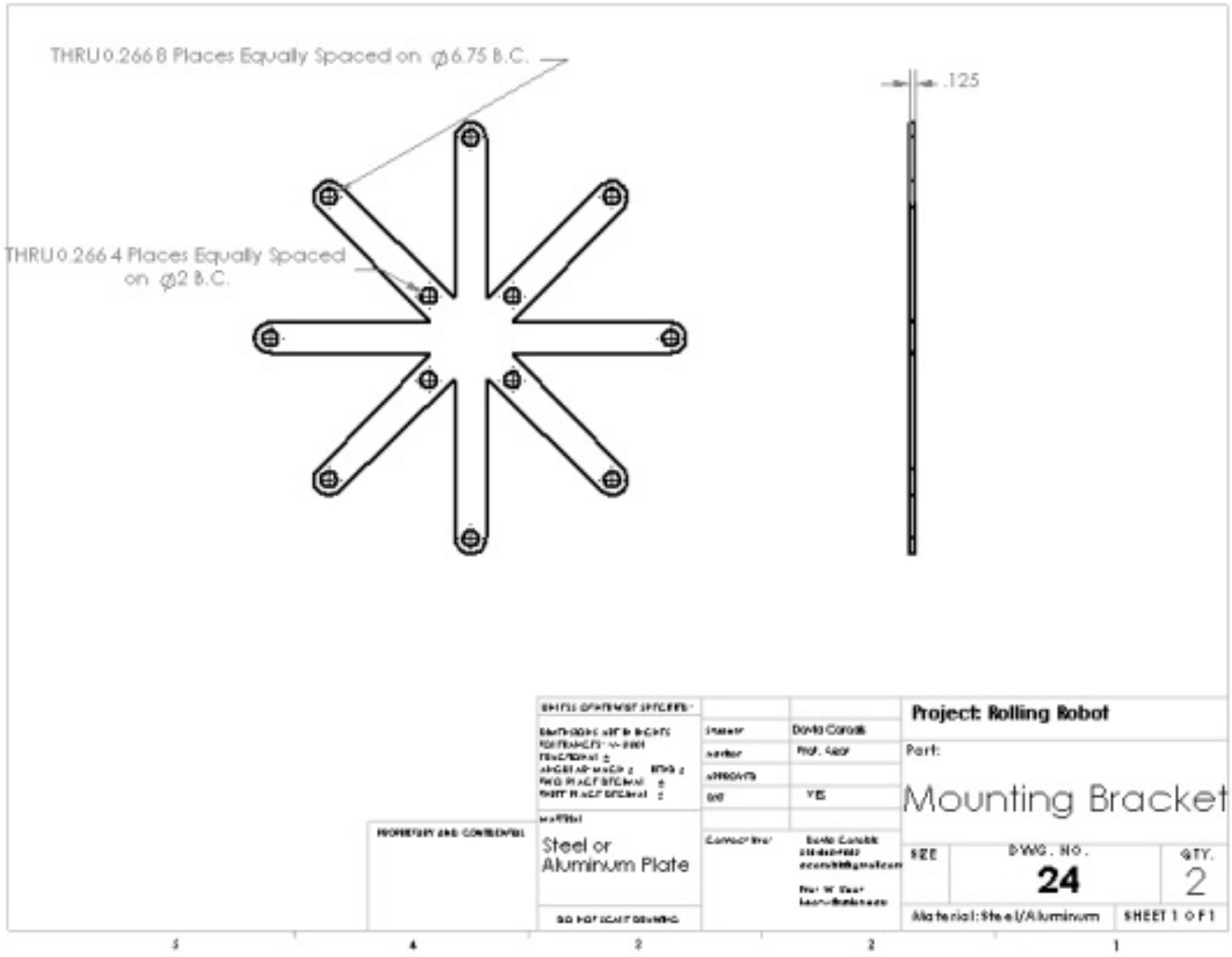
THRU 0.266 8 Places Equally Spaced on ⌀6.75 B.C.
THRU 0.266 4 Places Equally Spaced on ⌀2 B.C.
.125
Steel or Aluminum Plate
Project: Rolling Robot
Part:
Mounting Bracket
SIZE
DWG. NO.
24
QTY.
2
Material: Steel/Aluminum
SHEET 1 OF 1

Item No.	Part	QTY
3	Shell Assembly	1
23	Internal Components Assembly	1
24	Mounting Bracket	2
E	1/4-20 Machine Screw	24

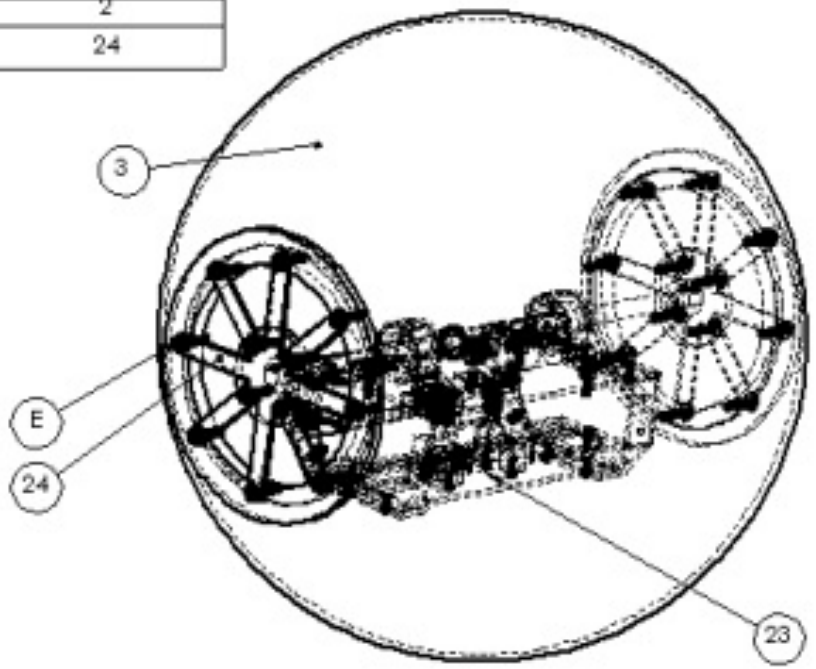

Project: Rolling Robot

Part:

Full Assembly

SIZE | DWG. NO. 25 | QTY. 1

SHEET 1 OF 1

Appendix F - References

1. Popular Mechanics,

   http://www.popularmechanics.com/technology/engineering/robots/4332921

2. Robot-Kits.org website, *Zentra Robotic Creations*,

   http://robot-kits.org/category/a-morphing-hexapod/

3. *Engineering Mechanics, Statics & Dynamics, Twelth Edition,* R. C. Hibbeler

4. http://plastic-domes-spheres.com/plastic-spheres/

5. Petco website, http://www.petco.com

6. McMaster-Carr, online catalog, www.mcmaster.com

7. Precision Microdrives website, www.precisionmicrodrives.com